


Rhizosphere microbiome structure alters to enable wilt resistance in tomato

Min-Jung Kwak^{1,8}, Hyun Gi Kong^{2,8}, Kihyuck Choi^{2,8}, Soon-Kyeong Kwon^{1,8}, Ju Yeon Song^{1,8}, Jidam Lee¹, Pyeong An Lee², Soo Yeon Choi², Minseok Seo^{3,7} , Hyoung Ju Lee², Eun Joo Jung², Hyein Park¹, Nazish Roy², Heeal Kim^{3,4}, Myeong Min Lee¹, Edward M Rubin^{5,7}, Seon-Woo Lee² & Jihyun F Kim^{1,6}

Tomato variety Hawaii 7996 is resistant to the soil-borne pathogen *Ralstonia solanacearum*, whereas the Moneymaker variety is susceptible to the pathogen. To evaluate whether plant-associated microorganisms have a role in disease resistance, we analyzed the rhizosphere microbiomes of both varieties in a mesocosm experiment. Microbiome structures differed between the two cultivars. Transplantation of rhizosphere microbiota from resistant plants suppressed disease symptoms in susceptible plants. Comparative analyses of rhizosphere metagenomes from resistant and susceptible plants enabled the identification and assembly of a flavobacterial genome that was far more abundant in the resistant plant rhizosphere microbiome than in that of the susceptible plant. We cultivated this flavobacterium, named TRM1, and found that it could suppress *R. solanacearum*-disease development in a susceptible plant in pot experiments. Our findings reveal a role for native microbiota in protecting plants from microbial pathogens, and our approach charts a path toward the development of probiotics to ameliorate plant diseases.

Plants have a genetically imprinted innate immune system that responds to microbe/pathogen-associated molecular patterns and pathogen effectors^{1–3}. Plants also have salicylate-mediated systemic acquired resistance, induced systemic resistance, physical barriers and phytochemicals^{4,5}. Disease development may also be affected by environmental factors, including commensal microbes, which either inhabit plant niches or live in soil. In *Arabidopsis thaliana*, salicylic acid shapes the root microbiome⁶, but a mechanistic role for plant microbiota in pathogen defense has not yet been established.

Plant roots absorb water and inorganic nutrients and secrete organic exudates^{7,8}. Every gram of soil in the rhizosphere that surrounds plant roots is estimated to contain billions of microorganisms that comprise tens of thousands of species; thus, soil is considered to be a highly complex and dynamic ecosystem^{9–11}. Plant-associated microbes are known to have important roles in plant health and disease^{12,13}, and several studies have reported microbial censuses of *Arabidopsis*, barley, corn, rice, soybean and wheat, among others^{14–20}.

To elucidate the structure and function of the plant microbiome in disease development, we used the tomato plant (*Solanum lycopersicum*) and bacterial wilt as a model system. Tomato is a member of the *Solanaceae* family and is a model plant for studying disease resistance²¹. Bacterial wilt, caused by the betaproteobacterium *Ralstonia solanacearum*, is a soil-borne disease that can infect hundreds of plant species, including *Solanaceae*^{22,23}. *R. solanacearum* enters the root

through wounds, root tips or cracks, colonizes the cortex, and invades xylem vessels. It spreads systemically and blocks water transport, which results in plant wilting and eventual death. In potato crops, this pathogen causes an estimated \$1 billion in losses annually worldwide²⁴. Host resistance remains the most effective control strategy for bacterial wilt, as is common with other soil-borne diseases²⁵.

We used *S. lycopersicum* var. Hawaii 7996, which is highly resistant to *Ralstonia* wilt, and Moneymaker, a tomato cultivar that is susceptible to the disease^{26,27}, to investigate the interactions between plant, pathogen and microbiota through comparative analyses of the rhizosphere microbiomes and subsequent functional evaluation of a cultured bacterium for its suppression of tomato wilt.

RESULTS

Structure of the tomato rhizosphere microbiome

First, we set up a mesocosm experiment with plots containing Hawaii 7996, Moneymaker, Korean cabbage or soil alone (**Supplementary Fig. 1** and Online Methods), and we used DNA prepared from the rhizosphere or bulk soil for amplicon sequencing of the V1–V3 region of the 16S ribosomal RNA gene and shotgun sequencing of the whole metagenome. Amplicon sequencing was performed in triplicate using samples from three independent experiments.

From the first round of 16S rDNA sequencing (**Supplementary Table 1a**), we obtained 12,486 ± 3,615 processed reads for each sample.

¹Department of Systems Biology, Division of Life Sciences, and Institute for Life Science and Biotechnology, Yonsei University, Seoul, Republic of Korea.

²Department of Applied Biology, Dong-A University, Busan, Republic of Korea. ³C&K Genomics, Seoul, Republic of Korea. ⁴Department of Agricultural Biotechnology and Research Institute of Agriculture and Life Sciences, Seoul National University, Seoul, Republic of Korea. ⁵Department of Energy Joint Genome Institute (DOE JGI) and Lawrence Berkeley National Laboratory, Berkeley, California, USA. ⁶Strategic Initiative for Microbiomes in Agriculture and Food (iMAF), Yonsei University, Seoul, Republic of Korea. ⁷Present addresses: Channing Division of Network Medicine, Harvard Medical School and Brigham and Women's Hospital, Boston, Massachusetts, USA (M.S.) and Metabiota Inc., San Francisco, California, USA (E.M.R.). ⁸These authors contributed equally to this work. Correspondence should be addressed to J.F.K. (jfk1@yonsei.ac.kr) or S.-W.L. (seonlee@dau.ac.kr).

Received 21 June 2017; accepted 1 August 2018; published online 8 October 2018; doi:10.1038/nbt.4232

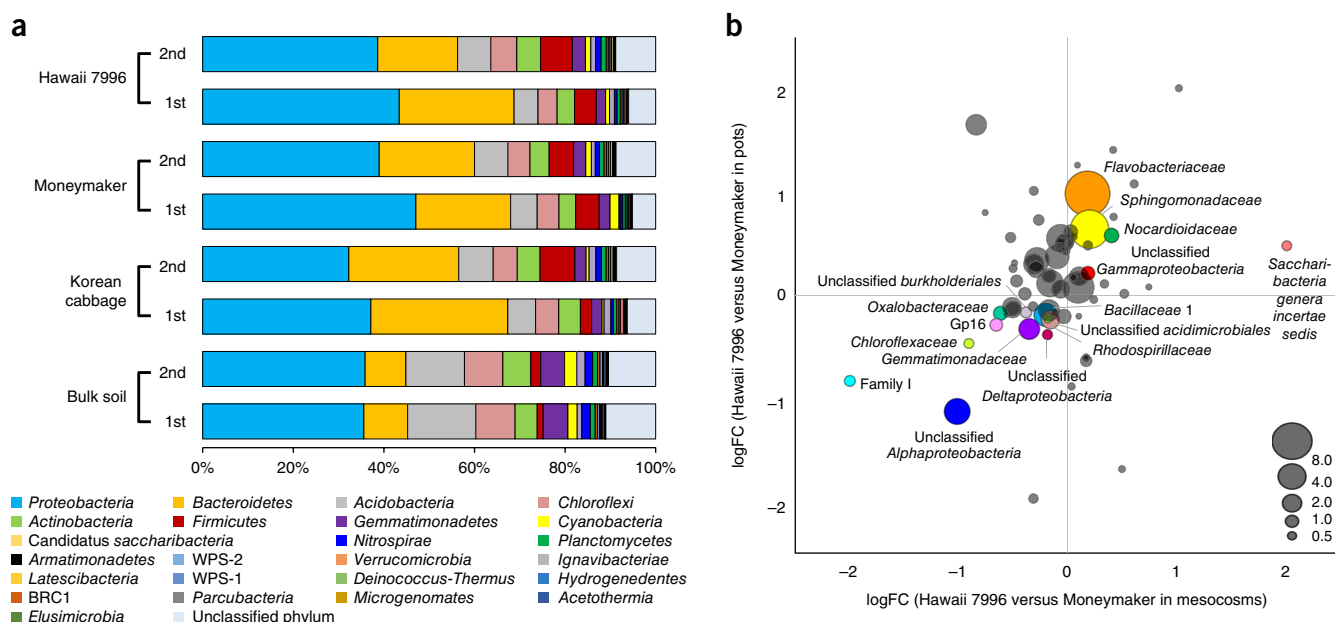


Figure 1 Comparison of the soil community structures in the mesocosm experiment based on pyrosequencing of 16S rDNA amplicons. **(a)** Taxonomic comparison at the phylum level. First sample: communities in the active growth and the first flowering stage; second sample: communities in the fruiting and senescence stage. **(b)** Correlation of relative abundances at the family level between Hawaii 7996 and Moneymaker in the mesocosm and pot experiments. The x axis and the y axis display log-transformed fold change of the normalized relative abundance between the plants grown in mesocosms or pots, respectively. The plot shows 67 bacterial families with $\geq 0.1\%$ relative abundance and average relative abundance values were indicated by circle size. Colored circles are the families that have the relative abundance of ≥ 0.5 and the logFC value of ≥ 0.15 or ≤ -0.15 in both of the experiments.

The number of operational taxonomic units (OTUs) at 97% sequence identity ranged from 1,952 to 5,134. Species richness indices indicated that the number of OTUs in the plant rhizosphere was reduced compared with bulk soil samples (**Supplementary Fig. 2a,b**). In all of the samples analyzed, species richness was reduced in the first sampling (during prolific plant growth and the first flowering) compared with the second sampling (during fruiting and senescence). Similarly, species evenness or the similarity of each OTU in relative abundance was reduced during active growth (**Supplementary Fig. 2b**). There were substantial differences in the bacterial community structures of bulk and planted soils: of the 24 phyla that we detected, the relative abundance of eight phyla was significantly different between bulk and planted soils (FDR adjusted P value ≤ 0.05 ; **Supplementary Table 2a**). In the bulk soil, *Proteobacteria*, *Acidobacteria*, unclassified phylum, *Bacteroidetes*, *Chloroflexi*, *Actinobacteria* and *Gemmatimonadetes* were among the main phyla detected (**Fig. 1a**). In contrast, *Bacteroidetes* (logFC, FDR adjusted P value: 1.88, 3.81×10^{-21}), *Firmicutes* (2.22, 3.87×10^{-7}), *Verrucomicrobia* (1.78, 1.09×10^{-4}), *Ignavibacteriae* (1.59, 2.28×10^{-3}), *Proteobacteria* (0.73, 1.09×10^{-2}) and *BRC1* (1.40, 4.63×10^{-2}) were present in significantly increased proportions in the rhizosphere compared with bulk soil, whereas the abundance of *Acidobacteria* (-0.52 , 1.92×10^{-2}) and *Gemmatimonadetes* (-0.54 , 2.10×10^{-2}) was reduced.

The differences among the rhizosphere communities were more pronounced during active growth and flowering than in senescence, and, for tomato rhizosphere samples, between the two sampling times than the two cultivars (**Supplementary Fig. 2c**). Abundant phyla in tomato included *Proteobacteria*, *Bacteroidetes*, *Acidobacteria*, unclassified phylum and *Firmicutes* (**Fig. 1a**), and proportions of unclassified *Proteobacteria* (logFC, FDR adjusted P value: 1.80, 2.68×10^{-8}), *Flavobacteriia* (0.90, 8.92×10^{-3}), *Alphaproteobacteria* (0.63, 8.83×10^{-2}) and *Betaproteobacteria* (0.72, 8.83×10^{-2}) were higher in

the growing and flowering stage (**Supplementary Table 2b**). When we compared the rhizospheres of Hawaii 7996 and Moneymaker at the first stage of growth, we noticed an outgrowth of *Bacteroidetes* in Hawaii 7996 (abundance in Hawaii 7996, logFC: 25.34%, 0.28) among the phyla with $\geq 1\%$ abundances. At the class and family levels, *Flavobacteriia* (16.67%, 0.32) and *Flavobacteriaceae* (16.25%, 0.30), as well as *Sphingomonadaceae* (9.95%, 0.32) and *Pseudomonadaceae* (1.19%, 0.40), appeared to be more abundant in Hawaii 7996 (**Supplementary Fig. 2d–f**) among those with populations higher in the rhizosphere than in bulk soil. In contrast, unclassified *Alphaproteobacteria* (abundance in Moneymaker, logFC: 7.15%, 0.90), unclassified *Proteobacteria* (4.06%, 0.72), *Comamonadaceae* (2.39%, 0.39) and *Oxalobacteraceae* (1.62%, 0.50), of which the latter two belong to *Betaproteobacteria* (6.65%, 0.35), seemed predominant in Moneymaker.

Repeat analyses of two additional 16S rDNA sequence datasets (second and third sequencing in **Supplementary Table 1a**), one of which was obtained from a pot experiment with the bulk soil used in the mesocosms, yielded similar results (Pearson correlation coefficients for phyla, classes, orders and families 0.87–0.99; **Supplementary Figs. 3 and 4**). For both the field and pot experiments, abundances of some families, such as *Flavobacteriaceae* (logFC, FDR adjusted P values for bulk soil versus Hawaii 7996/bulk soil versus Moneymaker: $3.91/3.34$, $8.66 \times 10^{-13}/1.77 \times 10^{-9}$), *Comamonadaceae* ($2.56/2.84$, $6.43 \times 10^{-6}/6.32 \times 10^{-7}$) and unclassified *Proteobacteria* ($2.89/2.42$, $4.44 \times 10^{-7}/1.40 \times 10^{-5}$), were more than twofold higher in the tomato rhizosphere during active plant growth and flowering than in bulk soil (**Supplementary Table 2c** and **Supplementary Fig. 2g,h**). In the rhizosphere of Hawaii 7996, *Flavobacteriaceae* and *Sphingomonadaceae* were non-statistically significantly increased compared with bulk soil (logFC ≥ 0.15), as were unclassified *Alphaproteobacteria*, *Oxalobacteraceae* and *Bacillaceae* in Moneymaker (**Fig. 1b**).

Although useful, 16S rDNA sequencing is subject to amplification bias. To complement our 16S data, we carried out shotgun sequencing of rhizosphere samples of Hawaii 7996 and Moneymaker during the growing and flowering stages (**Supplementary Table 1b**). We obtained 372,826,452 and 376,069,704 high-quality paired-end reads from Hawaii 7996 and Moneymaker, respectively, after trimming and removal of tomato sequences. We recruited 251,252 and 249,216 reads that matched the small-subunit rRNA gene using read alignment (**Supplementary Fig. 5a** and Online Methods) against the SILVA database. More than 80% of these reads were from Bacteria, >7% were from Eukarya and <5% were from Archaea. Among Bacteria, consistent with our amplicon sequencing data, *Flavobacteriia* was predominant in Hawaii 7996, whereas *Bacilli* and *Betaproteobacteria* were abundant in Moneymaker (**Supplementary Fig. 5b,c**).

To investigate the functional profiles of the rhizosphere microbiome, we assembled the metagenomic reads from Hawaii 7996 and Moneymaker into 1,257,840 and 1,229,497 scaffolds, respectively. Next, we predicted protein-coding sequences (CDSs) and identified 4,402,149 non-redundant CDSs from tomato rhizosphere metagenomes (**Supplementary Table 3**). We found that 4,180,636 and 4,165,753 CDSs matched the reads from Hawaii 7996 and Moneymaker, respectively. This suggests that both rhizospheres have comparable genetic diversity. 203,204 and 188,321 CDSs were only detected in Hawaii 7996 or Moneymaker, respectively. Comparison of taxonomic assignments of the CDSs specific to each rhizosphere revealed that *Flavobacteriia* CDSs were present in larger proportions in Hawaii 7996, and *Cyanobacteria* CDSs were dominant in Moneymaker (**Supplementary Figs. 5d** and **6a,b**). Assignment of Clusters of Orthologous Groups (COG)²⁸ categories to these CDSs further indicated that gene function categories were similar between the two cultivars (**Supplementary Fig. 6c**). However, CDSs belonging to 'translation, ribosomal structure and biogenesis (J)' were more abundant in Hawaii 7996, whereas those belonging to 'secondary metabolites biosynthesis, transport and catabolism (Q)' were more abundant in Moneymaker (**Supplementary Fig. 5e,f**).

Microbiota and disease development

Based on preliminary observations that the microbiome profiles of the rhizospheres of Hawaii 7996 and Moneymaker are distinct, we investigated whether the rhizosphere microbiota are associated with resistance or susceptibility to *Ralstonia*-induced wilt. First, we grew tomato cultivars into the field soil that had been used in our mesocosm experiment, transplanted them and inoculated them with *R. solanacearum* (Online Methods and **Fig. 2a**). Hawaii 7996 plants that were either transplanted into soil that Moneymaker had grown in, or replanted into soil that Hawaii 7996 had grown in, had similar patterns of symptoms over time (**Fig. 2b** and **Supplementary Fig. 7**). However, the symptoms progressed more quickly in Hawaii 7996 planted in Moneymaker soil (2 d faster). In contrast, the slope of disease progression was lower and disease severity was reduced 27.7% at day 14 in Moneymaker plants that were transplanted into soil that Hawaii 7996 had grown in compared with Moneymaker plants replanted into soil that Moneymaker had grown in.

Given that all of the pots into which gnotobiotic seeds were originally planted contained the same field soil, we hypothesized that the microbial communities present in the soil in which plants grew were fostered by the plant during cultivation. However, there are alternative explanations. Perhaps root exudates²⁹, rather than the rhizosphere microbiota, of Hawaii 7996 affect symptom development during *Ralstonia* infection. To explore the possibility that Hawaii 7996 or Moneymaker secrete root exudates that affect the growth of

R. solanacearum, we inoculated *Ralstonia* cells into a broth culture complemented with root exudates from each tomato lines (Online Methods). We observed no substantial effect of root exudates on bacterial growth in these conditions (**Supplementary Fig. 8a,b**). Although it is likely that root exudates of the two tomato lines differ in chemical composition, which would contribute to microbiota assemblage in the rhizosphere in a cultivar-dependent manner, we found no direct influence of root exudates on *R. solanacearum* growth.

We hypothesized that microbiota in the Hawaii 7996 rhizosphere delayed bacterial invasion and colonization of the xylem vessels. We next set out to test this hypothesis by analyzing whether flavobacteria in the Hawaii 7996 rhizosphere contribute to disease response in tomato. We isolated 477 different bacteria by dilution plating (Online Methods) and found that 31 strains of the flavobacteria that we cultivated had growth-promoting effects on tomato seedlings and/or growth-inhibiting activities against *Phytophthora infestans*, *Phytophthora capsici* or *Rhizoctonia solani* (Online Methods, **Supplementary Fig. 8c,d** and **Supplementary Table 4**). To our surprise, however, none of our flavobacterial isolates, including *Flavobacterium anhuiense* RCM74, *F. aquidurens* RC62, *F. beibuense* RSKm HC5, *F. daejeonense* RCH33 and *Flavobacterium* sp. TCH3-2, were antibacterial toward *R. solanacearum* on solid media, nor could any of these strains at a density of approximately 10⁷ CFU/g of soil suppress *Ralstonia* wilt in tomato after a soil drench application (Online Methods and data not shown).

Metagenomic assembly of a flavobacterial genome

Our metagenomics analyses revealed that *Flavobacteriaceae* species were dominant in the Hawaii 7996 rhizosphere microbiome, but the flavobacterial strains that we isolated were unable to antagonize *R. solanacearum* or suppress tomato wilt, at least under the conditions that we tested. Our comparative COG analyses of the gene pools in the rhizospheres of Hawaii 7996 and Moneymaker could not assign putative disease response functions to a specific taxon.

Next, we attempted to identify bacterial strains that might contribute to microbiota-related disease responses by assembling genomes from our metagenomic sequence data (**Supplementary Table 1b**). We classified scaffolds according to their taxonomic affiliation at the phylum level, as determined by 107 marker genes³⁰. Scaffold binning revealed that *Proteobacteria* and *Bacteroidetes* were the most dominant, as determined by the number of scaffolds and the sum of the scaffold lengths (**Supplementary Table 5**). We visualized scaffolds by color coding phyla and graphing these on the basis of G+C content and fold coverage. To our surprise, this revealed a cluster of *Bacteroidetes* scaffolds present in Hawaii 7996 (**Fig. 3a**). These scaffolds were not absent from the Moneymaker sample, but their coverage was greatly reduced.

We reassembled the reads present in the scaffolds with 30–40% G+C and 25–50× coverage into 388 contigs, which we examined for *Bacteroidetes* marker genes and aberrant coverage. After gap-filling the selected contigs, we were able to reconstruct a hypothetical flavobacterial genome from the tomato rhizosphere that comprised 57 contigs and was 4.11 Mb without rRNA operons; we named this genome TRG1 (tomato rhizosphere genome 1; **Fig. 3b** and **Supplementary Tables 6** and **7**). It is the first microbial genome assembled from the tomato rhizosphere to our knowledge. Phylogenomic analysis of 255 *Flavobacteriia* genomes and TRG1 using the sequences of 13 conserved proteins (Online Methods) placed TRG1 next to that of *Gaetbulibacter saemankumensis* DSM 17032 (**Fig. 3c**), and marked the strain(s) corresponding to TRG1 as a potentially new taxonomic division in *Flavobacteriaceae*.

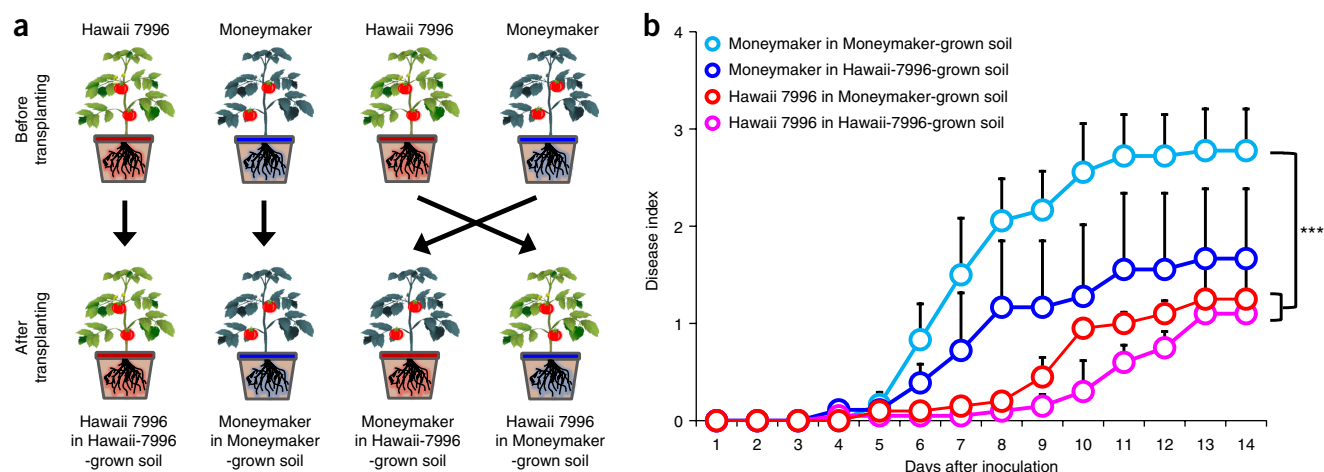


Figure 2 Transplant experiment of tomato cultivars and responses to *R. solanacearum*. (a) Experimental scheme of the rhizosphere microbiota translocation of Hawaii 7996 and Moneymaker. (b) Progress of *Ralstonia* wilt disease on transplanted tomato cultivars. Repeated measures ANOVA showed a significant difference between Moneymaker planted in Moneymaker-cultivated soil and Hawaii 7996 planted in either Moneymaker-cultivated soil or Hawaii-7996-cultivated soil ($***P < 0.001$), a significant difference between experimental period ($P < 2.2 \times 10^{-16}$), and a significant interaction between cultivar and experimental day ($P < 2.2 \times 10^{-16}$). However, there was no significant difference between Moneymaker planted in Moneymaker-cultivated soil and Moneymaker planted in Hawaii-7996-cultivated soil ($P = 0.1581$), a significant difference between experimental period ($P < 2.2 \times 10^{-16}$), and a significant interaction between cultivar and experimental day ($P = 1.059 \times 10^{-8}$). Given that we observed a significant interaction between treatment and experimental day, we further investigated with a separate test at specific experimental days (Supplementary Fig. 7). Each data point represents the mean disease index for three independent experiments ($n = 18$ in total for susceptible plants and $n = 20$ in total for resistant plants for each treatment). Each vertical bar represents the s.e.m. from three independent experiments.

Using reference genomes to infer flavobacterial functions

To better understand the putative functions of rhizosphere microbiome in tomato, we also adopted a reference genome-guided approach. Metagenomic reads of the two cultivars (Supplementary Table 1b) were mapped to 1,190 completely sequenced bacterial genomes (Online Methods). Of 168 genomes matched with $\geq 1\times$ genome coverage, none were *Flavobacteriia* (Supplementary Fig. 9a). When the same reads were mapped to 226 *Flavobacteriia* genomes that included draft sequences, TRG1 and the genomes of *F. daejeonense* RCH33 and DSM 17708 (ref. 31) matched with $\geq 1\times$ genome coverage. DSM 17708 was isolated from greenhouse soil in Korea. There were twice as many reads matching TRG1 in Hawaii 7996 as in Moneymaker (Fig. 3d), suggesting that the number of cells in Hawaii 7996 was proportionately higher. In contrast, the number of reads matching the RCH33 and DSM 17708 genomes was only slightly higher in Hawaii 7996, although the abundance of RCH33 sequences seemed comparable to that of TRG1.

We compared the gene contents of TRM1 (the presumptive uncultured microbe corresponding to TRG1) to eight marine isolates in the same clade as TRM1 and two soil isolates, RCH33 and DSM 17708, in the family (Supplementary Fig. 9b). TRM1 shared 1,199 genes with the eight marine isolates, comprising the core gene set of the lineage. TRM1 also had 128 'niche-specific' genes that were not present in the eight marine isolates, but that were common to the two soil isolates; most of these were in gene clusters and were predicted to encode proteins involved in carbohydrate metabolism or transport (Supplementary Fig. 9c and Supplementary Table 7). Analysis of the COG distribution also indicated that the three soil-borne *Flavobacteriaceae* strains had higher proportions of genes involved in 'carbohydrate metabolism and transport (G)' than the eight marine strains (Supplementary Fig. 9d). Categorization of the carbohydrate-associated enzymes using the CAZy database highlighted three genes encoding enzymes that degrade hemicellulose or pectin (GH43, GH28 and GH127) among those that were overrepresented in the soil strains (Supplementary Table 8).

TRM1 has nearly 1,000 taxon-specific genes, many of which are either clustered or in islands (Fig. 3b and Supplementary Table 7). In TRM1, there are 28 ECF sigma factors (Fig. 4a) for detecting environmental cues and 23 pairs of SusC/SusD for carbohydrate utilization (Fig. 4b), which might contribute to rhizosphere fitness. Gliding motility and the type IX (Por) secretion system, predicted from the genome data, might help TRM1 compete with other microbes in soil or even lyse them³². TRM1 has eight siderophore transport systems for iron acquisition and may synthesize phytase, rhodanese, acetolactate synthase, diacetyl reductase, tRNA dimethylallyltransferase and 1-aminocyclopropane-1-carboxylate deaminase (Supplementary Table 7) to promote plant productivity or immunity^{10,33,34}. In addition, there are at least eight acetyltransferases (COG5653, involved in cellulose biosynthesis; Supplementary Fig. 9e) and two genes each encoding fucose permease, mannose transporter, rhamnose permease and xylose transporter in TRG1.

Cultivation of TRM1

We attempted to cultivate TRM1 by combining TRG1 sequence information and metadata from the mesocosm experiment. We designed three sets of PCR primers for *rpoA*, *recA* and *secY* (Supplementary Table 9a and Supplementary Fig. 10a). For attempted cultivation, we chose marine broth (our phylogenomic analysis indicated that TRM1 had marine bacterial relatives) and diluted it 1:10 (v/v) to better suit slow growing organisms. We also tested artificial seawater supplemented with peptone as a growth medium. Inspection of the metabolic pathways suggested that TRM1 might use D-mannose as a sole carbon source, which turned out to be optimal for preparing the enriched cell stock (Supplementary Fig. 10b). We also note that TRM1 harbors a kanamycin-resistance gene. Using 1:10 diluted marine agar containing 2% NaCl and 30 $\mu\text{g/ml}$ kanamycin, we obtained 22 candidate TRM1 colonies (Supplementary Fig. 10c,d), of which one was a pink colony and the rest were yellow. All of the isolates were subject to PCR using the three TRM1-specific primers, and product sequences confirmed that they are TRG1 sequences (Supplementary Table 10).

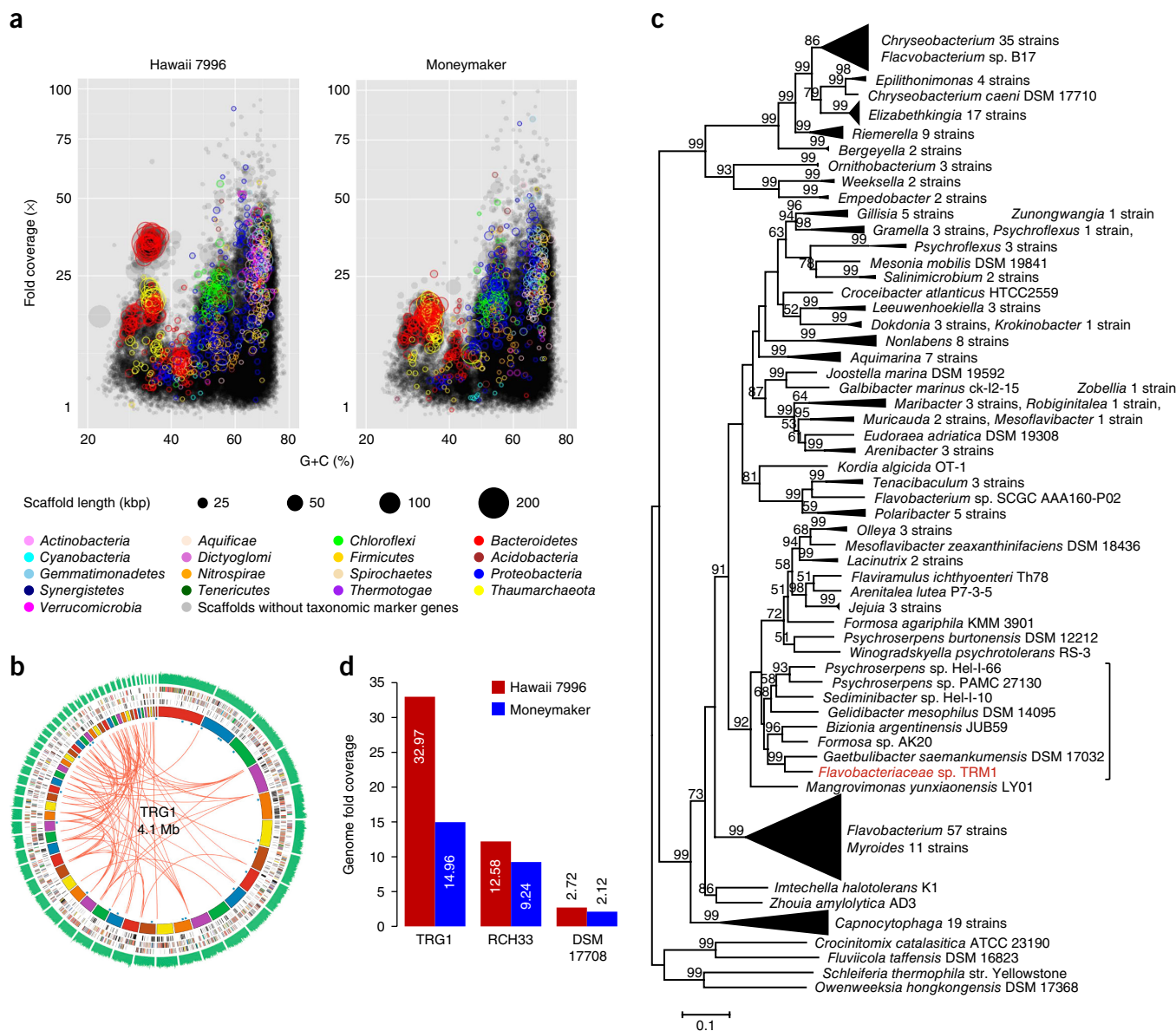


Figure 3 Scaffold binning and reconstruction of a metagenome-derived *Flavobacteriaceae* genome. **(a)** Clustering and taxonomic assignment of the scaffolds. Scaffolds were clustered according to the G+C content and fold-coverage of each scaffold. Taxonomic assignment was performed with phylum-level phylogenetic marker genes. Gray circles represent taxonomically unassigned scaffolds because of the absence of the marker genes. Black regions are a result of the overlap of numerous gray circles. **(b)** Circular representation of a reconstructed genome. The first circle from inside shows the 57 contigs sorted by size. The second circle represents 955 TRG1-specific genes shown in **Supplementary Figure 9b** and **Supplementary Table 7**. The third and fourth circles indicate COG-assigned genes in color codes. The fifth circle is for the G+C content. The innermost blue-scattered spots indicate the tRNA genes and the red lines indicate connections of paired-end reads at the end of each contig. **(c)** An unrooted phylogenetic tree of *Flavobacteriia* based on 13 proteins conserved in 255 genomes, which was constructed using the maximum likelihood method. **(d)** Fold-coverage of three *Flavobacteriaceae* genomes, which were detected with $\geq 1\times$ genome fold-coverage in whole-metagenome data.

We amplified and sequenced 16S rRNA genes for these 22 isolates and used these $\geq 99.39\%$ identical sequences (**Supplementary Table 10**) to infer the abundance of TRM1 in the field and pot samples. From the mesocosm experiment, the proportions of TRM1 sequences or those with $>97\%$ identity for 16S rDNA during the growing and flowering stage were calculated to be 2.46 and 2.25% (first and second sequencing) in Hawaii 7996 and 1.10 and 0.77% in Moneymaker among the amplicon sequence reads in each sample, whereas they were 0.63% in Hawaii 7996 and 0.36% in Moneymaker among the whole metagenome sequence reads (**Supplementary Table 11**). In contrast, the

abundances of TRM1 in Hawaii 7996 and Moneymaker were much lower during fruiting and senescence than in the earlier stage, and they were remained at almost undetectable levels (0–0.04%) in bulk soils. Similar observations were made with the pot samples. However, some bacterial taxa were present in all samples at similar abundance (for example, *Ohtaekwangia* strains $2.17 \pm 0.35\%$).

TRM1 and disease resistance

We tested whether TRM1-10 (**Fig. 5a,b**, and **Supplementary Fig. 10e**) could antagonize *R. solanacearum* on plates or suppress bacterial wilt

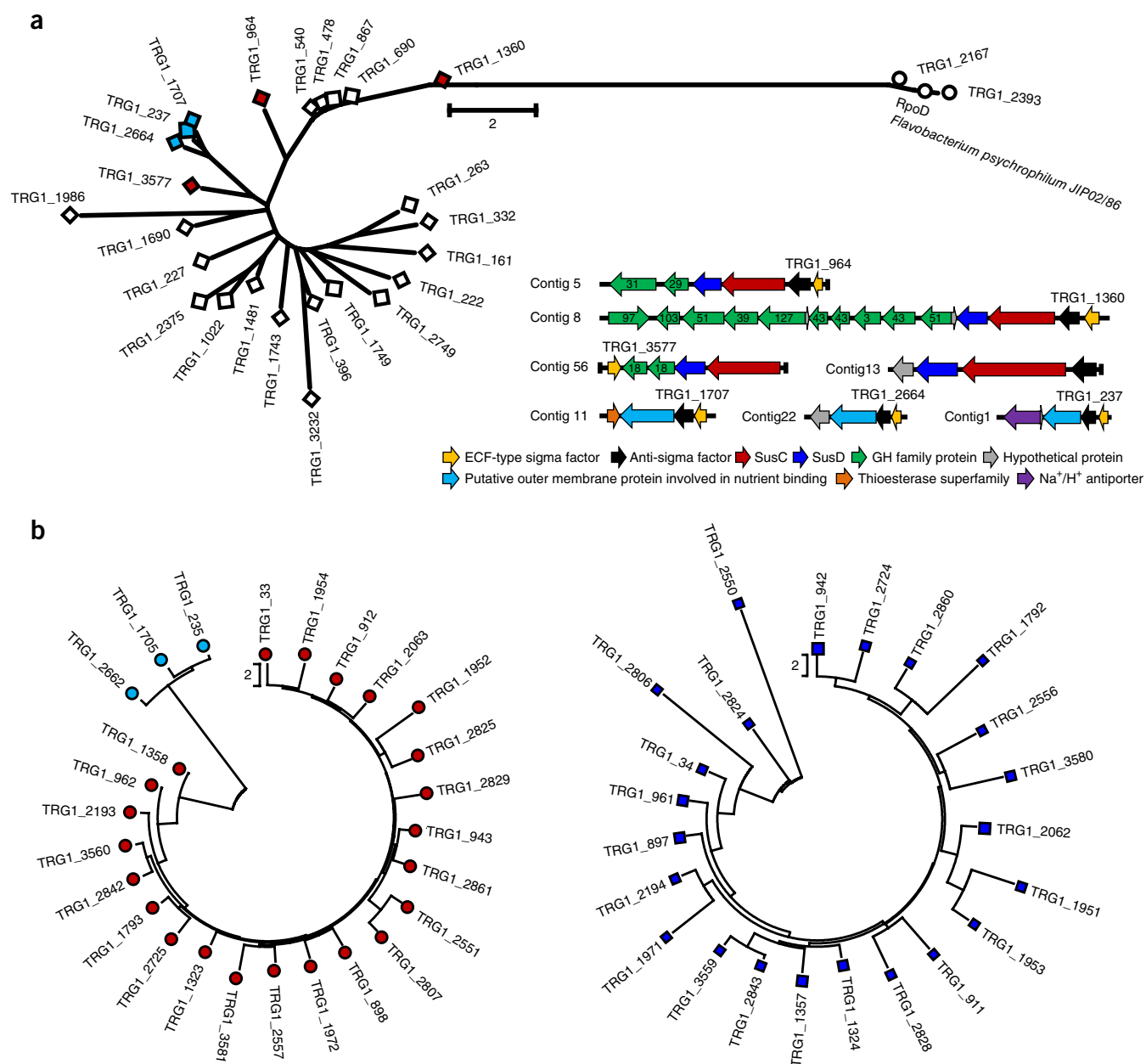


Figure 4 Sigma factors and starch utilization system proteins in TRM1. Neighbor-joining trees were constructed using a Jones–Taylor–Thornton matrix-based method using the amino acid sequences of each gene. **(a)** A radiation tree of the σ^{70} family of sigma factors. Among the 28 sigma factors in TRG1, TRG1_3374 was not included in the tree construction because of its short length. Open circles represent RpoD and an RpoD homolog. Diamonds indicate ECF-type sigma factors. Red diamonds indicate sigma factors whose encoding genes are located next to the anti-sigma factor gene and *susC/susD*. Among the *susC/susD* pairs, one was detected at one end of contig 13 with an anti-sigma factor gene but no sigma factor gene. Sky-blue diamonds indicate sigma factors whose encoding genes are next to an anti-sigma factor gene and a gene encoding a putative outer membrane protein involved in nutrient binding. Numbers in the green arrows represent the numbers of glycoside hydrolase families. **(b)** Circle trees of SusC and SusD. Red circles indicate SusC and blue squares are SusD. In the genome of TRM1, 23 pairs of *susC/susD* were detected. Sky-blue circles indicate putative outer membrane proteins involved in nutrient binding, which correspond to the sky-blue genes indicated in **a**. In TRG1, dozens of other genes contain the SusC domain region, but their functions are apparently unrelated to starch utilization.

symptoms in tomato. The antagonistic activity of TRM1-10 against *R. solanacearum* was examined by the zone of inhibition assay (Online Methods). We were unable to observe the growth inhibition of *R. solanacearum* by TRM1-10 (data not shown). TRM1-10 at approximately 2×10^8 CFU/g of soil was poured to soak the base of 2-week-old Moneymaker plants grown in autoclaved horticultural nursery soil. A week later, the plants were inoculated with *R. solanacearum*, and

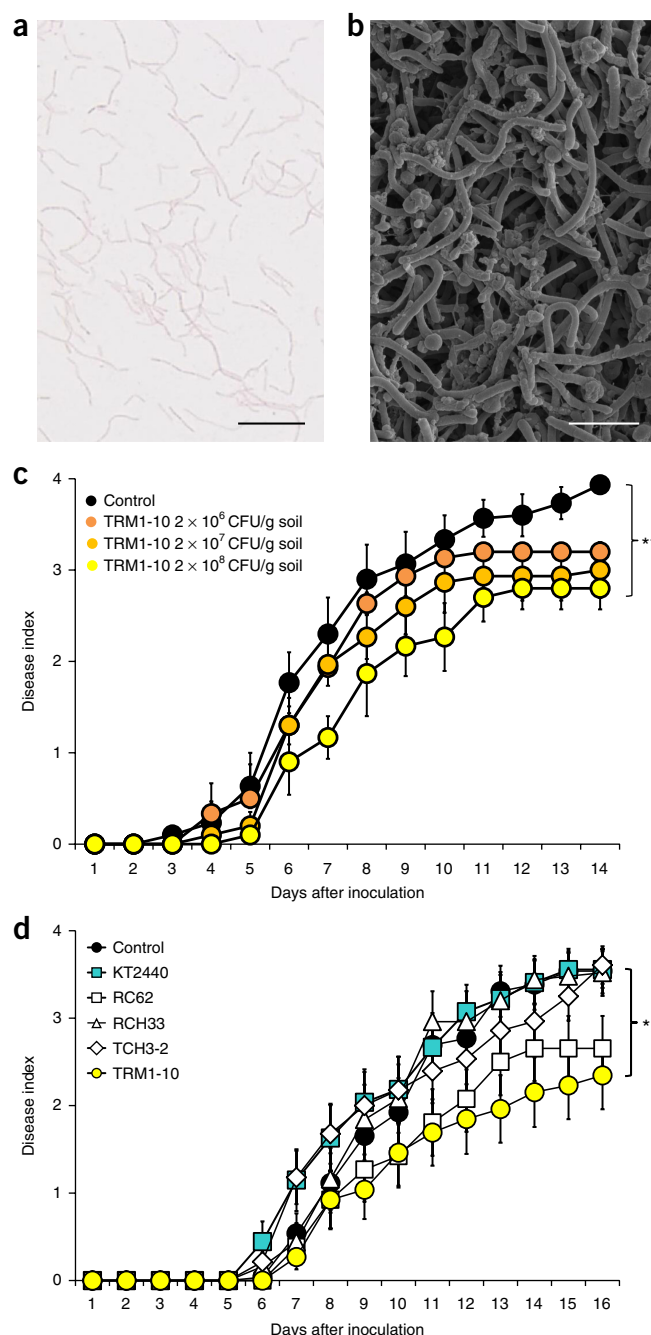
disease symptoms were monitored for 2 weeks. Significant suppression of the progress of bacterial wilt was noted when compared with the untreated control ($P < 0.01$ by repeated measures ANOVA; **Fig. 5c** and **Supplementary Fig. 11**). However, application of TRM1-10 at approximately 2×10^6 or 2×10^7 CFU/g of soil did not significantly suppress wilt symptoms ($P > 0.05$), suggesting that TRM1-10-mediated suppression of the bacterial wilt progress is dose dependent.

Figure 5 *Flavobacteriaceae* strain TRM1-10 and its effect on the progress of bacterial wilt in Moneymaker. **(a)** Microscopic image of TRM1-10 cells grown on a marine agar plate. Scale bar indicates 10 μm . **(b)** Scanning electron micrograph of TRM1-10 cells grown on a marine agar plate. Scale bar indicates 2.5 μm . **(c)** Disease progress of bacterial wilt on Moneymaker treated with TRM1-10 in sterile nursery soil. Repeated measures ANOVA showed a significant difference between TRM1-10 treatment at a high density (2×10^8 CFU/g of soil) and control treatment ($**P = 0.0039714$), a significant difference between experimental periods ($P = 2.2 \times 10^{-16}$), and a significant interaction between treatments and experimental days ($P = 0.0004604$). However, there was no significant difference between TRM1-10 treatment at a lower density (2×10^7 and 2×10^6 CFU/g soil) and the control treatment ($P = 0.088$ and 0.371 , respectively). **(d)** Disease progress of bacterial wilt on Moneymaker treated with TRM1-10, *F. aquidurens* RC62, *F. daejeonense* RCH33, *Flavobacterium* sp. TCH3-2 or *P. putida* KT2440 in non-sterile nursery soil. Repeated measures ANOVA displayed a significant difference between TRM1-10 treatment and control treatment in non-sterile nursery soil ($*P = 0.03775$). Treatment of each of the *Flavobacterium* strains was not significantly different from the non-treatment control for bacterial wilt suppression. Significant interaction between TRM1-10 treatment and experimental days were noticed ($P = 3.081 \times 10^{-6}$). Each data point represents the mean disease index from three independent experiments containing 30 plants in total for each treatment. Each vertical bar represents the s.e.m. from three replicates (each replicate with 10 plants, $n = 30$).

Some flavobacteria including *F. aquidurens* RC62, *F. daejeonense* RCH33 and *Flavobacterium* sp. TCH3-2 (Supplementary Table 12) have been shown to have growth-promoting effects on tomato in our study, and *Pseudomonas putida* KT2440 can induce systemic resistance in *Arabidopsis* and maize against a bacterial or fungal disease, respectively^{35,36}. We compared the biocontrol activity of TRM1 and these bacteria for their ability to suppress disease on Moneymaker plants grown in non-sterile or sterile soils, using the same soil drench method (Online Methods). TRM1-10 suppressed bacterial wilt in non-sterile soil (Fig. 5d and Supplementary Fig. 12a), whereas none of the other strains tested suppressed bacterial wilt. In sterile soil, TRM1 and *P. putida* KT2440 both suppressed bacterial wilt symptoms (Supplementary Fig. 12b).

We further investigated population dynamics of TRM1-10 and *R. solanacearum* in plants grown in sterile horticultural nursery soil (Online Methods and Fig. 6a). The total number of cells, live or dead, was estimated using DNA copy numbers measured by quantitative real-time PCR (qPCR; primers listed in Supplementary Table 9b) and culturable cells were enumerated by colony counting. Overall, qPCR detected more cells than colony counting, but there was concordance between the two ($r = 0.91$, $p = 2.2 \times 10^{-16}$ for TRM1-10; $r = 0.70$, $P = 2.9 \times 10^{-5}$ for *R. solanacearum*; Supplementary Fig. 13a). The population of TRM1-10 in the rhizosphere of Hawaii 7996 treated with TRM1-10 at approximately 2×10^8 CFU/g soil gradually declined for 1 week to stabilize at approximately $2.48 \pm 0.79 \times 10^6$ to $2.67 \pm 3.07 \times 10^6$ total or cultured cells/g soil, whereas for Moneymaker TRM1 the population declined to $1.06 \pm 0.48 \times 10^5$ to $1.44 \pm 1.17 \times 10^4$ total or cultured cells/g soil, by 10 d and then recovered to $1.81 \pm 0.82 \times 10^5$ to $3.44 \pm 3.17 \times 10^4$ cells/g soil by 2 weeks (Fig. 6b,d and Supplementary Table 13). Numbers of TRM1-10 in bulk soil of Hawaii 7996 were maintained, albeit at $2.62 \pm 1.06 \times 10^5$ cultured cells/g soil, by 2 weeks, compared with $5.26 \pm 5.33 \times 10^5$ cultured cells/g soil in the rhizosphere, whereas in Moneymaker the numbers of TRM1-10 declined to $3.33 \pm 4.71 \times 10^2$ cultured cells/g soil and three of five replicates could not be cultivated by 2 weeks (Supplementary Fig. 13b).

Notably, the TRM1-10 population in the rhizosphere of Moneymaker treated with TRM1-10 followed by approximately 1×10^7 CFU *R. solanacearum*/g soil was more than threefold higher than



that in Moneymaker treated with TRM1-10 alone at 1 week (Fig. 6c). The TRM1-10 population was increased by 3 h post *R. solanacearum* inoculation, but there was no statistically significant difference in cell counts at any time point, except for qPCR estimation at 3 h ($P = 0.015$). Unlike in Moneymaker treated with TRM1-10 alone ($P = 0.039$ in 3 h, $P = 3.9 \times 10^{-4}$ in 3 d, $P = 0.003$ in 7 d), when *R. solanacearum* was present, TRM1-10 was found in the bulk soil of Moneymaker at levels similar to that in Hawaii 7996 (Moneymaker 1.17×10^6 , Hawaii 7996 1.99×10^6 cultured cells/g soil at day 7; Supplementary Fig. 13b). The population of *R. solanacearum* in the rhizosphere of TRM1-10-treated Moneymaker, in contrast, rapidly dropped just 3 h after inoculation compared with *R. solanacearum* applied in the absence of TRM1 (Fig. 6e,f), whereas the number in bulk soil was slightly lower than that at inoculation (Supplementary Fig. 13b). Over the next 7 d,

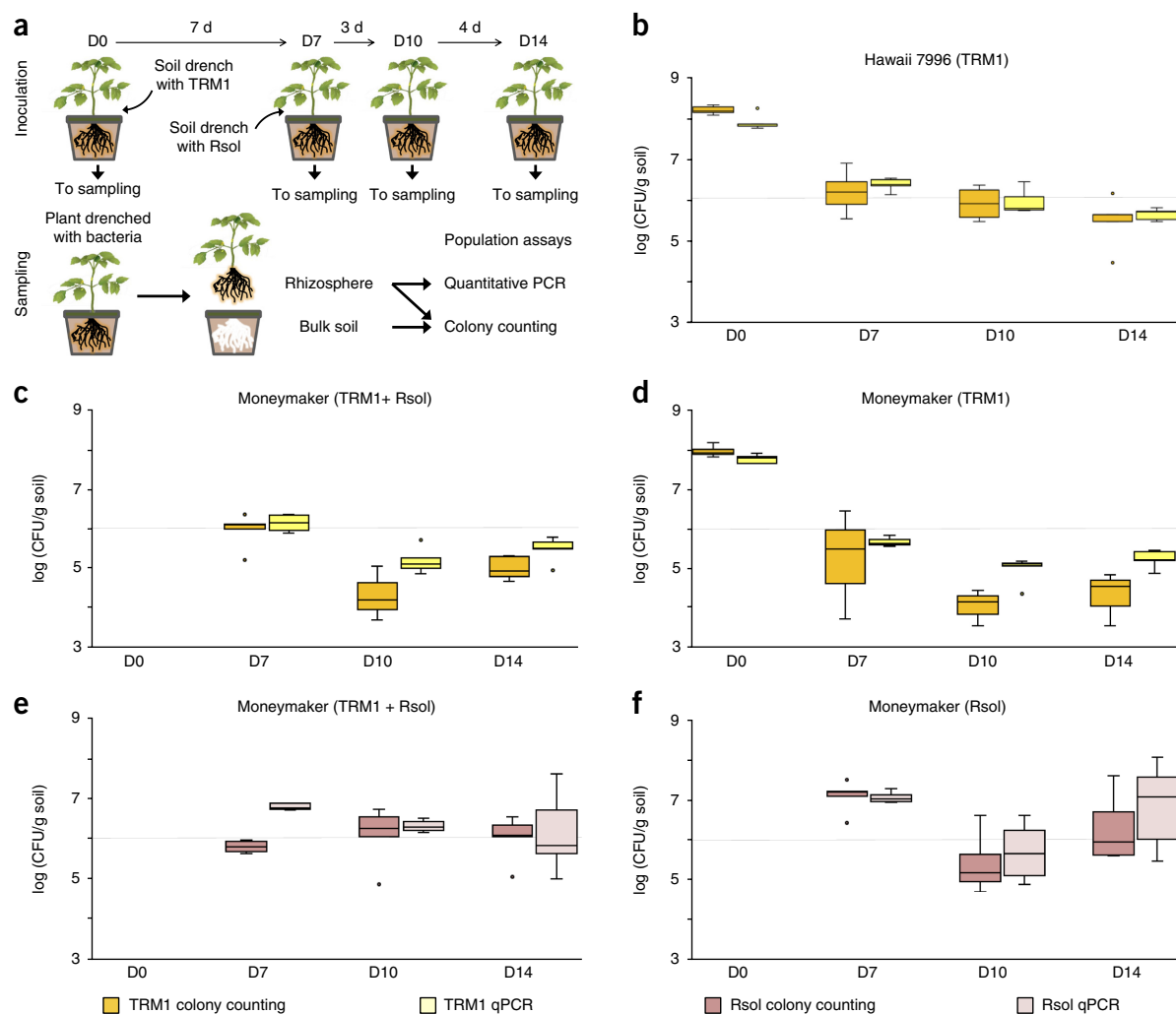


Figure 6 Population dynamics of TRM1-10 and *R. solanacearum* in Hawaii 7996 and Moneymaker. **(a)** Experimental scheme for sampling of rhizospheric and bulk soils for colony counting and qPCR. TRM1, TRM1-10; Rsol, *R. solanacearum*. **(b)** Population change of TRM1-10 in the rhizosphere of Hawaii 7996 over time. **(c,d)** Population changes of TRM1-10 in the rhizospheres of Moneymaker with or without *R. solanacearum* inoculation. **(e,f)** Population changes of *R. solanacearum* in the rhizospheres of Moneymaker with or without TRM1-10 pretreatment. Boxes indicate interquartile range (75 to 25% of the data, $n = 5$) and the median value is shown as a line in the box. Outliers are represented by dots. Two-sample, two-sided t tests were used to compare bacterial populations between samples. The mean of five replications ($n = 5$) for colony counting results showed significantly higher populations of TRM1-10 in Hawaii 7996 compared with Moneymaker on day 10 (D10, $P = 0.005$) and D14 ($P = 0.028$), but no significant difference was observed on D7 ($P = 0.290$). qPCR data revealed similar results; the populations of TRM1-10 were significantly higher on D7 ($P = 0.0008$), D10 ($P = 0.006$) and D14 ($P = 0.037$) in Hawaii 7996 than in Moneymaker. *R. solanacearum* population in Moneymaker inoculated with *R. solanacearum* alone was significantly higher than that in Moneymaker pre-treated with TRM1-10 ($P = 0.0001$ by colony count; $P = 0.01$ by qPCR) 3 h after *R. solanacearum* inoculation. However, the populations of *R. solanacearum* remained similar on both D10 and D14 and not significantly different with or without TRM1-10 pretreatment. *In planta*, *R. solanacearum* population in Moneymaker treated with *R. solanacearum* alone was higher (Supplementary Table 13).

the population level of *R. solanacearum* was maintained at about 2×10^6 CFU/g soil in the rhizosphere of Hawaii 7996, whereas the *R. solanacearum* population in the rhizosphere of Moneymaker treated with *R. solanacearum* alone decreased initially and increased after 3 d, as the endophytic population in infected plants began to build up (Supplementary Fig. 13c).

DISCUSSION

Bacterial wilt resistance is mediated by quantitative trait loci, but crop performance is variable and is influenced by environmental factors³⁷, which may include plant microbiota. Plants have a core rhizosphere microbiome, and plant genotype is thought to have a minor role in shaping microbiota composition compared with soil type^{14,15}.

One interpretation of our results is that specific microbial taxa may preferentially colonize the rhizospheres of Hawaii 7996 and Moneymaker and have important roles in disease response. Our study has limitations: we only carried out one mesocosm experiment and one pot experiment with five technical replications. Nevertheless, two independent microbiota analyses and one metagenome analysis provided consistent data. We hypothesize that plant genotype-specific tailoring of rhizosphere microbiota from the soil milieu may be driven by selection and coevolution of soil-borne strains⁶, but more evidence is required to support our hypothesis.

We found that disease-resistant tomatoes may recruit bacterial allies to protect themselves from infection. Our findings differ from those of studies using disease-suppressive soil^{38–40}, in which plants

are disease susceptible and disease severity is reduced as a result of changes in the microbiome profile in response to pathogen build-up, as specific microbial taxa are enriched in the resistant plant. Our results may be specific to soils for tomato cultivation. Soils are heterogeneous and it is not clear whether similar bacterial species would be present in different soils; more data are needed to make our results generalizable.

The tomato cultivars that we used have similar phenotypic traits, including root morphology, but have different reproductive tissues, for example, flowering pattern, flower clustering, fruit morphology and disease responses, such as bacterial wilt resistance^{26,27}. However, the biochemical or molecular bases for rhizosphere assemblage of microbiota in these cultivars has not been studied. We hypothesize that one or more quantitative trait loci in Hawaii 7996 may have a role in recruiting specific microorganisms that can promote resistance against bacterial wilt.

We successfully assembled the genome of an uncultured flavobacterium from the incredibly complex tomato rhizosphere metagenome using a taxonomic binning method^{30,41}. Our results reveal that flavobacteria such as TRM1 may have a beneficial role in defending host plants against bacterial diseases. Flavobacteria thrive in the ocean, freshwater or soil as plankton, nutrient recyclers, commensals and pathogens⁴². Genomic features of TRM1 associated with carbohydrate metabolism and other functions may assist in adaptation to life in the tomato rhizosphere and in protecting the tomato against *Ralstonia*. The presence of specific monosaccharide transporters raises the tantalizing possibility that the uptake of monosaccharides by TRM1 reduces the availability of sugars to which *R. solanacearum* lectin binds and thereby reduces infection^{43–46}.

A culture collection of *Arabidopsis* microbiota representing most bacterial species that are reproducibly detected was recently established using careful selection of media and growth conditions⁴⁷. Cultivation of TRM1 was achieved by exploiting knowledge gained from the TRG1 sequence information and rhizosphere metadata. One of our isolates, TRM1-10, was capable of suppressing disease symptoms of *Ralstonia*-infected susceptible tomatoes. We would caution that it is possible that TRM1 comprises a collection of closely related strains, such as TRM1-1–TRM1-22.

The rhizosphere microbiota may have a probiotic effect⁴⁸ on plant functions. Our study further supports assertions that the genetic basis of disease resistance posits the hologenome of the host and its microbial counterpart(s)^{49,50} as an important component of plant defense.

METHODS

Methods, including statements of data availability and any associated accession codes and references, are available in the [online version of the paper](#).

Note: Any Supplementary Information and Source Data files are available in the online version of the paper.

ACKNOWLEDGMENTS

We would like to thank members of the laboratories of J.F.K. and S.-W.L., including B.K. Kim, K.Y. Baek, T.-H. Kang, S. Kim, H.G. Lee, S.Y. Lee, G.J. Son, S. Yoo and H. Yu, as well as KRIBB-KOBIC and NABIC, for technical support, and Y.-S. Bahn, D. Choi, S.-Y. Kwon, I. Lee, W.-J. Lee and H.-S. Pai for helpful comments and suggestions. This study was financially supported by the Strategic Initiative for Microbiomes in Agriculture and Food (914001-4 to J.F.K. and 914006-4 to J.Y.S.), the Cooperative Research Program for Agricultural Science & Technology Development (PJ01093901 to S.-W.L.), the National Research Foundation (NRF-2014M3C9A33068822 and NRF-2011-0017670 to J.F.K.), and the Next-Generation BioGreen 21 Program (PJ008201 to S.-W.L.) of the Republic of Korea. Publication was supported in part by the Brain Korea 21 PLUS program, and M.-J.K., S.-K.K. and J.L. are fellowship awardees of the program.

AUTHOR CONTRIBUTIONS

J.F.K. and S.-W.L. conceived, organized and supervised the project. J.F.K., S.-W.L., M.M.L. and E.M.R. interpreted the results and prepared the manuscript. People in the laboratory of S.-W.L. performed the plant experiments; those in J.F.K.'s lab. analyzed the metagenomic data. M.-J.K. worked on the metagenome analysis, reconstructed TRG1, and drafted the microbiome results. H.J.L. contributed to setting up the plant experiment. H.G.K. and K.C. extracted the metagenomic DNA and analyzed the pyrosequencing data. J.Y.S. carried out the comparative analysis on field and pot experiments. M.S. and H.K. performed the statistical analysis for community structures. S.Y.C. and E.J.J. performed the transplant experiment as well as the isolation and phenotypic characterization of flavobacteria. K.C. and P.A.L. tested the influence of root exudates on bacterial growth. J.Y.S. annotated TRG1. M.-J.K., S.-K.K., and J.L. analyzed the genome information. J.L. and M.-J.K. isolated and characterized TRM1. P.A.L., J.L., and K.C. tested its effect as well as those of other flavobacteria on disease progress. Finally, S.-K.K., P.A.L., and N.R. performed the qPCR analysis. K.C., P.A.L., H.P., and N.R. enumerated cultured bacteria. J.F.K. composed the main text. J.F.K., S.-W.L., and M.-J.K. edited the manuscript. All of the authors read and approved the final version of the manuscript before submission.

COMPETING INTERESTS

The authors declare no competing interests.

Reprints and permissions information is available online at <http://www.nature.com/reprints/index.html>. Publisher's note: Springer Nature remains neutral with regard to jurisdictional claims in published maps and institutional affiliations.

- Dangl, J.L., Horvath, D.M. & Staskawicz, B.J. Pivoting the plant immune system from dissection to deployment. *Science* **341**, 746–751 (2013).
- Jones, J.D. & Dangl, J.L. The plant immune system. *Nature* **444**, 323–329 (2006).
- Hacquard, S., Spaepen, S., Garrido-Oter, R. & Schulze-Lefert, P. Interplay between innate immunity and the plant microbiota. *Annu. Rev. Phytopathol.* **55**, 565–589 (2017).
- Agrios, G. *Plant Pathology* (Elsevier Academic Press, Burlington, Massachusetts, USA, 2005).
- Pieterse, C.M. *et al.* Induced systemic resistance by beneficial microbes. *Annu. Rev. Phytopathol.* **52**, 347–375 (2014).
- Lebeis, S.L. *et al.* Salicylic acid modulates colonization of the root microbiome by specific bacterial taxa. *Science* **349**, 860–864 (2015).
- Taiz, L., Zeiger, E., Møller, I.M. & Murphy, A. *Plant Physiology and Development* 761 (Sinauer Associates, Sunderland, Massachusetts, USA, 2015).
- Hacquard, S. *et al.* Microbiota and host nutrition across plant and animal kingdoms. *Cell Host Microbe* **17**, 603–616 (2015).
- Bulgarelli, D., Schlaeppi, K. & Spaepen, S. Ver Loren van Themaat, E. & Schulze-Lefert, P. Structure and functions of the bacterial microbiota of plants. *Annu. Rev. Plant Biol.* **64**, 807–838 (2013).
- Mendes, R., Garbeva, P., Raaijmakers, J.M. The rhizosphere microbiome: significance of plant beneficial, plant pathogenic, and human pathogenic microorganisms. *FEMS Microbiol. Rev.* **37**, 634–663 (2013).
- Philippot, L., Raaijmakers, J.M., Lemanceau, P. & van der Putten, W.H. Going back to the roots: the microbial ecology of the rhizosphere. *Nat. Rev. Microbiol.* **11**, 789–799 (2013).
- Berg, G., Rybakova, D., Grube, M. & Köberl, M. The plant microbiome explored: implications for experimental botany. *J. Exp. Bot.* **67**, 995–1002 (2016).
- Castrillo, G. *et al.* Root microbiota drive direct integration of phosphate stress and immunity. *Nature* **543**, 513–518 (2017).
- Lundberg, D.S. *et al.* Defining the core *Arabidopsis thaliana* root microbiome. *Nature* **488**, 86–90 (2012).
- Bulgarelli, D. *et al.* Revealing structure and assembly cues for *Arabidopsis* root-inhabiting bacterial microbiota. *Nature* **488**, 91–95 (2012).
- Bulgarelli, D. *et al.* Structure and function of the bacterial root microbiota in wild and domesticated barley. *Cell Host Microbe* **17**, 392–403 (2015).
- Müller, D.B., Vogel, C., Bai, Y. & Vorholt, J.A. The plant microbiota: systems-level insights and perspectives. *Annu. Rev. Genet.* **50**, 211–234 (2016).
- Busby, P.E. *et al.* Research priorities for harnessing plant microbiomes in sustainable agriculture. *PLoS Biol.* **15**, e2001793 (2017).
- Leach, J.E., Triplett, L.R., Argueso, C.T. & Trivedi, P. Communication in the Phytobiome. *Cell* **169**, 587–596 (2017).
- Walters, W.A. *et al.* Large-scale replicated field study of maize rhizosphere identifies heritable microbes. *Proc. Natl. Acad. Sci. USA* **115**, 7368–7373 (2018).
- Tomato Genome Consortium. The tomato genome sequence provides insights into fleshy fruit evolution. *Nature* **485**, 635–641 (2012).
- Hayward, A.C. Biology and epidemiology of bacterial wilt caused by *Pseudomonas solanacearum*. *Annu. Rev. Phytopathol.* **29**, 65–87 (1991).
- Mansfield, J. *et al.* Top 10 plant pathogenic bacteria in molecular plant pathology. *Mol. Plant Pathol.* **13**, 614–629 (2012).
- Elphinstone, J.G. *Bacterial wilt disease and the Ralstonia solanacearum species complex* 9–28 (APS Press, St. Paul, Minnesota, USA, 2005).
- Huet, G. Breeding for resistances to *Ralstonia solanacearum*. *Front. Plant Sci.* **5**, 715 (2014).

26. Wang, J.F. *et al.* Resistance of tomato line Hawaii7996 to *Ralstonia solanacearum* Pss4 in Taiwan is controlled mainly by a major strain-specific locus. *Mol. Plant Microbe Interact.* **13**, 6–13 (2000).
27. Wu, J. *et al.* Loss of glutamate dehydrogenase in *Ralstonia solanacearum* alters dehydrogenase activity, extracellular polysaccharide production and bacterial virulence. *Physiol. Mol. Plant Pathol.* **90**, 57–64 (2015).
28. Galperin, M.Y., Makarova, K.S., Wolf, Y.I. & Koonin, E.V. Expanded microbial genome coverage and improved protein family annotation in the COG database. *Nucleic Acids Res.* **43**, D261–D269 (2015).
29. Hu, L. *et al.* Root exudate metabolites drive plant-soil feedbacks on growth and defense by shaping the rhizosphere microbiota. *Nat. Commun.* **9**, 2738 (2018).
30. Albertsen, M. *et al.* Genome sequences of rare, uncultured bacteria obtained by differential coverage binning of multiple metagenomes. *Nat. Biotechnol.* **31**, 533–538 (2013).
31. Kim, B.Y. *et al.* *Flavobacterium daejeonense* sp. nov. and *Flavobacterium suncheonense* sp. nov., isolated from greenhouse soils in Korea. *Int. J. Syst. Evol. Microbiol.* **56**, 1645–1649 (2006).
32. Banning, E.C., Casciotti, K.L. & Kujawinski, E.B. Novel strains isolated from a coastal aquifer suggest a predatory role for flavobacteria. *FEMS Microbiol. Ecol.* **73**, 254–270 (2010).
33. Naseem, M., Kaltdorf, M. & Dandekar, T. The nexus between growth and defense signaling: auxin and cytokinin modulate plant immune response pathways. *J. Exp. Bot.* **66**, 4885–4896 (2015).
34. Aznar, A. & Dellagi, A. New insights into the role of siderophores as triggers of plant immunity: what can we learn from animals? *J. Exp. Bot.* **66**, 3001–3010 (2015).
35. Matilla, M.A. *et al.* *Pseudomonas putida* KT2440 causes induced systemic resistance and changes in *Arabidopsis* root exudation. *Environ. Microbiol. Rep.* **2**, 381–388 (2010).
36. Planchamp, C., Glauser, G. & Mauch-Mani, B. Root inoculation with *Pseudomonas putida* KT2440 induces transcriptional and metabolic changes and systemic resistance in maize plants. *Front. Plant Sci.* **5**, 719 (2015).
37. Wang, J.F. *et al.* Identification of major QTLs associated with stable resistance of tomato cultivar ‘Hawaii 7996’ to *Ralstonia solanacearum*. *Euphytica* **190**, 241–252 (2013).
38. Mendes, R. *et al.* Deciphering the rhizosphere microbiome for disease-suppressive bacteria. *Science* **332**, 1097–1100 (2011).
39. Weller, D.M., Raaijmakers, J.M., Gardener, B.B. & Thomashow, L.S. Microbial populations responsible for specific soil suppressiveness to plant pathogens. *Annu. Rev. Phytopathol.* **40**, 309–348 (2002).
40. Cha, J.Y. *et al.* Microbial and biochemical basis of a *Fusarium* wilt-suppressive soil. *ISME J.* **10**, 119–129 (2016).
41. Sangwan, N., Xia, F. & Gilbert, J.A. Recovering complete and draft population genomes from metagenome datasets. *Microbiome* **4**, 8 (2016).
42. Buchan, A., LeCleir, G.R., Gulvik, C.A. & González, J.M. Master recyclers: features and functions of bacteria associated with phytoplankton blooms. *Nat. Rev. Microbiol.* **12**, 686–698 (2014).
43. Valls, M., Genin, S. & Boucher, C. Integrated regulation of the type III secretion system and other virulence determinants in *Ralstonia solanacearum*. *PLoS Pathog.* **2**, e82 (2006).
44. Genin, S. & Denny, T.P. Pathogenomics of the *Ralstonia solanacearum* species complex. *Annu. Rev. Phytopathol.* **50**, 67–89 (2012).
45. Meng, F., Babujee, L., Jacobs, J.M. & Allen, C. Comparative transcriptome analysis reveals cool virulence factors of *Ralstonia solanacearum* race 3 biovar 2. *PLoS One* **10**, e0139090 (2015).
46. Wei, Z. *et al.* Trophic network architecture of root-associated bacterial communities determines pathogen invasion and plant health. *Nat. Commun.* **6**, 8413 (2015).
47. Bai, Y. *et al.* Functional overlap of the *Arabidopsis* leaf and root microbiota. *Nature* **528**, 364–369 (2015).
48. Kim, J.F. *et al.* Genome sequence of the polymyxin-producing plant-probiotic rhizobacterium *Paenibacillus polymyxa* E681. *J. Bacteriol.* **192**, 6103–6104 (2010).
49. Bordenstein, S.R. & Theis, K.R. Host biology in light of the microbiome: ten principles of holobionts and hologenomes. *PLoS Biol.* **13**, e1002226 (2015).
50. Arnold, C. The hologenome: A new view of evolution. *New Sci.* **2899**, 30–34 (2013).

ONLINE METHODS

Tomato growth and soils. Tomato cultivars Moneymaker and Hawaii 7996 (ref. 51) were used as susceptible and resistant cultivars to bacterial wilt, respectively. Tomato seeds were surface-sterilized serially in 70% ethanol for 1 min, in 1% sodium hypochlorite solution for 15 min, and were finally rinsed extensively in sterile water five times. Surface-sterilized seeds of tomato cultivars were germinated in sterile water and planted into pots filled with soils. Except for a mesocosm experiment and a transplant experiment, tomato plants were grown in commercial horticulture nursery medium (Punong) as potting soil. When necessary, the nursery media were sterilized by autoclave twice (40 min each). For bacterial population analysis and bacterial wilt response, tomato plants were grown for 3–4 weeks in a controlled growth chamber at 28 °C in light for 14 h and in the dark for 10 h.

Experimental setup and sampling. To analyze the influence of rhizosphere microbial communities on the susceptibility of tomato cultivars to bacterial wilt, seedlings of tomato cultivars were transplanted in plastic houses at Dong-A University Agricultural Experimental Station, Busan, Korea (N 35.239°, E 128.978°).

Plants were grown in the plastic house from Oct. 14 to Nov. 17, 2011 (Supplementary Fig. 1). Soil conditions at this time were the following: pH, 7.0; EC, 39.50 ds/m; salinity, 2.53%; organic matter, 2.62%; total N, 0.15 mg/kg; total P, 1,037.00 mg/kg; P₂O₅, 545.26 mg/kg; Ca, 1,688.00 mg/kg; Mg, 216.50 mg/kg; K, 106.90 mg/kg; Na, 289.80 mg/kg; total microbes, 4.3×10^7 CFU/g dry soil; soil texture, silt loam. The first root samples of tomato (Nov. 1) were collected at the active growth and first flowering stage, and the second sampling (Nov. 14) was conducted at the fruiting and senescence stage. Rhizosphere soils from Korean cabbage were collected on the same days.

Plants grown in the plastic house were taken out from the field using a spade. Soils loosely attached to the plant roots were removed by gentle shaking, and soils tightly associated with plant roots were separated by vigorous vortexing in a sterile diluent (composition per liter: NaCl, 4.25 g; KH₂PO₄, 0.15 g; Na₂HPO₄, 0.3 g; MgSO₄, 0.1 g; gelatin, 0.05 g). The separated soil solution was centrifuged at 8,000 rpm for 10 min to collect rhizosphere soils. The collected soils from five plants were pooled and stored at –80 °C until use for microbial community analysis. In the same period, the tomato plants were also grown in a pot with the same field soil in a greenhouse, and five tomato plants were used for rhizosphere soil sampling following the same procedure. Metagenomic DNA from the rhizospheric soil was extracted using a FastDNA Spin kit for soil DNA (MP Biomedicals). As control samples, metagenomic DNAs from the bulk soil and the rhizosphere of Korean cabbage or hot pepper were also extracted.

16S rDNA amplicon sequencing and metagenome shotgun sequencing. For the community analysis, a portion of the 16S rRNA genes were amplified with barcoded universal primers (27F-GAGTTTGATCMTGGCTCAG and 518R-WTTACCGCGGCTGCTGG) spanning ~500 bp of the V1–V3 regions of the 16S rRNA gene. The primers used to amplify 16S rRNA gene are listed in Supplementary Table 14. Amplified PCR product was further processed to purify and pyrosequence at Macrogen and the National Instrumentation Center for Environmental Management (NICEM) in Korea. PCR products were sequenced by using the GS-FLX Titanium pyrosequencer (454 Life Sciences) at Macrogen and NICEM. For the whole metagenome analysis, rhizosphere samples of Hawaii 7996 and Moneymaker collected at the active growth and first flowering stage (Nov. 1) were selected, and metagenomic DNA was sequenced using a 500 bp paired-end library with HiSeq 2000 of Illumina/Solexa platform (one lane per sample) at Macrogen.

Quality and length trimming of the reads were conducted using the CLC Genomics Workbench 5.1 (CLC Bio) with 0.01 quality score, no ambiguities nucleotide, and 300-base minimum length. Homopolymer errors were removed using CD-HIT-OUT, and chimera sequences were removed with UCHIME after NAST (Nearest Alignment Space Termination) alignment against the SILVA database in the mothur pipeline. Read information is described in Supplementary Table 1a.

From the HiSeq 2000, a total of 491,280,606 reads for Hawaii 7996 and 484,700,526 reads for Moneymaker were generated. For trimming of the sequencing reads, the CLC Genomics Workbench 5.1 was used with the

parameters of 0.05 quality score, no ambiguities nucleotide, and 60-base minimum length. BMTagger⁵² was used for the removal of contamination of tomato genome sequences (accession number: AEKE000000000). Information on the sequencing reads is described in Supplementary Table 1b.

Community analysis based on the 16S rRNA gene. Taxonomic assignment of the high-quality reads was conducted using the RDP classifier 2.9 (Supplementary Table 15). Among the taxonomically assigned reads, the reads with a confidence estimate of more than 0.5 were assigned to the specific taxa. For the calculation of diversity indices, unique sequences were extracted at the 3% dissimilarity level. Using these unique sequences, calculation of rarefaction, abundance-based coverage estimators (ACE), Chao estimator, Jackknife estimator, Shannon index, and Inverse Simpson index, as well as construction of a distance matrix and clustering, were conducted using the mothur pipeline. For Principal coordinate analysis (PCoA), representative sequences at the 3% dissimilarity level were extracted from each sample, and the final PCoA result was generated with weighted UniFrac.

For the community analysis using whole metagenome data, the reads of the 16S rRNA gene were extracted from whole metagenome sequences. To recruit the 16S rDNA reads from whole metagenome sequences, the Burrows-Wheeler Aligner (BWA) was used with the parameter of 20 of maximum edit distance⁵², and the SILVA database (updated on Apr. 15, 2015, release SILVA Release 119) was used as a reference for the small-subunit rRNA gene. Taxonomic assignment of the selected reads was conducted with the RDP-Classifer⁵³.

To statistically analyze the abundances of individual operational taxonomic units, Trimmed Mean of M values normalization was performed in each taxonomic count data to consider different library size⁵⁴. For considering three-way factorial design, the Analysis of Deviance (ANODEV) model was employed for significance test between trials at each taxonomic rank from phylum to family. In addition, the negative-binomial assumption was considered as a response variable to solve the over-dispersion problem in count data⁵⁵. Under the diverse null hypothesis, likelihood ratio test was performed with a contrast matrix on the three-way ANODEV model. The probability values were adjusted by false discovery rate (FDR) multiple testing adjustment. Here, 5% significance level was considered as a significant result. The statistical test was performed using edgeR implemented in R⁵⁶.

De novo assembly and annotation of metagenomic reads. For the gene content analysis, *de novo* assembly of the whole metagenomic reads was performed with the CLC Assembly Cell (ver. 4.0.6) with the parameter of 25 word size and 300-bp minimum contig/scaffold length at the National Agricultural Biotechnology Information Center (NABIC) in Korea.

The prokaryotic gene prediction was conducted with MetaGeneMark⁵⁷, and redundant genes were removed using CD-HIT⁵⁸ with the parameters of 95% coverage and 90% identity⁵². After removal of the redundant genes, the whole metagenomic reads were mapped to non-redundant genes using BWA with the parameter of 20 of maximum edit distance, and the abundance of the each gene was calculated as reads per kilobase (RPK); RPK = No. of mapped reads / length of reference genomes in kb (length/1,000). Functional categorization of the genes was conducted with COG database using RPS-BLAST with the parameter of 1×10^{-2} of *e* value⁵⁹. Functional assignment of the genes was conducted using the NR database and BLASTP with the parameter of 1×10^{-4} of *e* value.

Transplant experiment of tomato plants. To investigate the influence of rhizosphere microbial community on plant characteristics such as bacterial wilt resistance in tomato, we examined the bacterial wilt resistance of a tomato cultivar growing with a disturbed microbial community in the rhizosphere. The basic idea was to transplant tomato cultivars into different microbial communities and inoculate *Ralstonia solanacearum* SL341 (race 1, biovar 3, phylotype I)⁶⁰ into those plants to evaluate the effect of the altered microbial community on bacterial wilt resistance. Surface-sterilized seeds of the tomato cultivars Moneymaker and Hawaii 7996 were germinated in a pot with sterilized (autoclaved twice) nursery media (Punong) and transferred into a pot with field soil from the experimental plots used for microbial community analysis of the tomato rhizosphere. For transplantation, the grown tomato plants were carefully taken out from the pot, leaving most of the rhizosphere soils behind; this was done by gently crushing the soil adhering to the

tomato roots. The pulled roots of tomato plants were washed thoroughly in a water bath sonicator for 5 min to remove most of the rhizosphere soils. The removed rhizosphere soil slurries were returned to the original pots in which the uprooted tomato plants were grown. The plants were then replanted either into pots with the soils in which the same cultivar was grown or into pots with soils in which a different cultivar was grown (Fig. 2a). Three days after transplantation and replantation, *R. solanacearum* was inoculated into the plants by soil-soaking inoculation⁶⁰. Bacterial inoculum of *R. solanacearum* SL 341 was prepared as previously described⁶⁰. The prepared bacterial suspensions were poured into a pot to reach the bacterial concentration of 1×10^7 CFU/g of soil. All inoculations included 5–10 plants for each experimental pot, and the non-inoculated plants were the negative controls. The inoculation experiments were repeated three times. Plants were monitored for disease progress over time after inoculation, and bacterial wilt was rated using the following scale: 0, no wilting; 1, 1–25% leaves wilted; 2, 25–50% leaves wilted; 3, 51–75% leaves wilted; 4, 76–100% leaves wilted⁶¹. Repeated measures analysis of variance was performed with the original data of percentage of wilted leaf of tomato using R (version 3.2.0).

Isolation of root exudates and co-cultivation with *R. solanacearum*. Tomato cultivars were cultivated in sterilized nursery media for three weeks and carefully removed from the pot and washed gently. Then, six plants were transferred to an Erlenmeyer flask with 150 ml of sterilized distilled water, shaded, aerated and maintained for 10 h at 25 °C. The water with root exudates were collected and filtered through membrane filter (diameter 0.22 µm). The filter sterilized root exudate was collected again until 5 times. The root exudate broth was prepared by mixing 5 ml of 5 × M9 broth with 20 ml of root exudate. Some of the root exudate broth was supplemented with glucose to have final concentration of 2%. Two negative controls included the M9 broth with soil aqueous extract of nursery soil or just the equivalent volume of sterile water. For preparation of soil aqueous extract, 1 g of sterilized nursery soil in 100 ml of sterile water was added, shaken, and aerated for 10 h at 25 °C. The suspension was centrifuged and filter-sterilized to collect the soil extract. *R. solanacearum* SL341 was inoculated in the root exudate broth and grown at 28 °C by vigorous shaking. The absorption at 600 nm and colony forming units were examined every 10 h up to 70 h.

Identification of flavobacterial isolates from the rhizospheric soil. Rhizosphere soil from mesocosm plots was suspended into diluent solution (composition per liter: NaCl, 4.25 g; KH₂PO₄, 0.15 g; Na₂HPO₄, 0.3 g; MgSO₄, 0.1 g; gelatin, 0.05 g) and the soil suspension was dilution spread onto 0.5× tryptic soy agar (TSA) medium or R2A medium⁶² supplemented with 0.2% sodium pyruvate. The primers used to detect bacterial isolates of flavobacteria were designed by multiple alignment of 16S rRNA genes of *Flavobacteriaceae* retrieved from GenBank. Among those 16S rRNA genes, 77 sequences with ≥1,400 bp were aligned by CLUSTALW by using ‘genefisher2’ provided at <http://bibiserv.techfak.uni-bielefeld.de/genefisher2> (ref. 63). Four forward primers and four reverse primers were selected and tested on various soil isolates of different taxa (list not shown). Bacterial cells were subject to colony PCR with primers fsp1f (5′-TTTCGCAAGACAATTACAAGG-3′) and fsp2r (5′-TTACCAAGTTTACCCTAGGCAG-3′), and annealing at 58 °C. Selected bacterial colonies were further identified by sequence determination of the full-length 16S rRNA gene amplified by PCR. Finally, selected isolates were frozen at –80 °C and stored to be used for further characterization.

Phenotypic characterization of flavobacterial isolates. Isolated flavobacterial strains (Supplementary Table 4) were used to investigate bacterial characteristics. Antibiotic resistance was determined by colony development on TSA medium supplemented with various antibiotics. Antibacterial activity of the isolates against *R. solanacearum* was evaluated by coculturing flavobacterial isolates on CPG plate lawn covered by *R. solanacearum*. Bacterial growth inhibition, as indicated by an inhibition zone, was recorded as the anti-*R. solanacearum* effect. Antifungal activity of the isolates was investigated against *Rhizoctonia solani*, *Phytophthora capsici* and *Phytophthora infestans*. *R. solani* was co-cultured on TSA medium with flavobacteria, and *P. capsici* and *P. infestans* were co-cultured with flavobacteria on V8 juice medium (composition per liter: V8 juice, 200 ml; CaCO₃, 4.3 g). Fungal growth inhibition

was determined by the hyphal growth inhibition zone on the media. Cellulase activity was tested by growing flavobacterial isolates on the TSA medium supplemented with 1% carboxymethyl cellulose (CMC).

Effects of the isolates on plant growth and wilt resistance. Seedling growth of tomato cultivar Hawaii 7996 was investigated by planting germinated seedlings in pots with sterile nursery media and in pots with the field soil collected from the plastic houses used for the mesocosm study. Bacterial suspension was prepared to have 1.0 OD_{600nm} and tomato seeds were germinated in a sterile Whatman filter paper soaked with the bacterial suspension. Germinated seedlings were planted into either the sterile commercial nursery media or field soil for 7 d, and the bacterial suspension was poured into the pots at a density of 10^7 cells/g soil. Control experiments included tomato seeds germinated in sterile water and maintained under the same condition as the treated plants. Plant growth was evaluated three to 5 weeks after growth in a pot by removing soils on the roots and measuring the lengths of plants as well as their fresh and dry weights. Each treatment included ten plants and each experiment was replicated twice. Flavobacteria isolated from this trial were also examined for bacterial wilt suppression as described above.

Reconstruction of a novel flavobacterial genome. To identify the bacterial origin of each scaffold, we used a previously described method³⁰. For the binning of each scaffold, G+C content and tetranucleotide frequency of each scaffold were calculated, and 107 single-copy marker genes⁶⁴ were used for the taxonomic assignment of the scaffolds. First, the scaffolds were clustered according to the G+C content and scaffold fold-coverage. After clustering of the scaffolds, the taxonomic assignment of each scaffold was conducted using the information of existence of the marker genes⁶⁵. These results were plotted using R script and the scaffolds of specific taxa were extracted for further analysis. The CDSs from the extracted scaffolds were functionally classified using RPS-BLAST against the COG database with the *e* value cutoff of 1×10^{-2} .

To reconstruct the unknown genome of interest from the whole metagenome sequences, the paired-end reads mapped to the scaffolds—which are clustered by 20 to 40% G+C content and 25–50× fold-coverage—were extracted. The extracted paired-end reads were reassembled using the CLC Genomics Workbench 5.5.1 with default parameters. After re-assembly, the contigs with aberrant coverage or with the taxonomic marker gene of best hit with the non-flavobacterial gene were removed. Next, the gaps between the contigs were filled with the CLC Genomics Workbench using the information of paired-end reads at the end of the contigs. Genome circle of the reassembled genome was constructed with circos and scripts from the multi-metagenome pipeline⁶⁴. To avoid possible contamination, k-mer frequencies are considered when the contigs are assembled. Contigs with aberrant coverage or with the taxonomic marker gene of best hit with the non-flavobacterial gene were further removed (Online Methods). According to MIMAG standards⁶⁵, TRG1 is a high-quality draft with completeness score 98.68% and contamination score 1.30%.

To find the closest bacterial group of the reassembled genome, the average nucleotide identity based on BLAST was calculated with Jspecies using 273 genomes of *Flavobacteriia*, which included the draft genomes of *Flavobacterium anhuiense* RCM74, *F. aquidurens* RC62, *F. beibuense* RSKm HC5, *F. daejeonense* RCH33 and *Flavobacterium* sp. TCH3-2 isolated in this study. To identify the phylogenetic position of this reassembled genome, a phylogenomic tree was constructed using 13 conserved proteins: dTDP-glucose 4,6-dehydratase (TRG1_1083), YebC/PmpR family DNA-binding transcriptional regulator (TRG1_1649), DNA mismatch repair protein MutL (TRG1_2629), manganese superoxide dismutase (TRG1_1339), thioredoxin reductase (TRG1_876), SufE family protein (TRG1_626), transcription termination protein NusA (TRG1_1149), thymidylate synthase (TRG1_2295), peptidyl-tRNA hydrolase (TRG1_3211), 16S rRNA (guanine(527)-N(7))-methyltransferase RsmG (TRG1_2131), SsrA-binding protein SmpB (TRG1_1467), 50S ribosomal protein L7/L12 (TRG1_411), DUF2795 domain containing protein (TRG1_3254). For construction of a phylogenomic tree, the broadly conserved genes in 255 *Flavobacteriia* strains (Supplementary Table 16) were identified using OrthoMCL (version 2.0.3) with parameters of *e* value ≤ 1×10^{-5} , identity ≥ 50%, and coverage ≥ 50%. The amino-acid sequences of each conserved gene in 255 *Flavobacteriia* were aligned using MUSCLE (ver. 3.6) and 13 alignment

files were concatenated to an alignment file. After this, an un-rooted maximum likelihood tree was constructed using MEGA (ver. 5.10) with the Jones-Taylor-Thornton model for calculating evolutionary distances, 1,000 replications of bootstrap, and the complete-gap deletion method.

Comparative analyses of the assembled genome. For comparative analysis of the reassembled TRG1 genome with genome-determined bacterial strains, completely sequenced bacterial genomes were collected from the NCBI ftp. Among 2,264 genomes, the genomes of 1,190 strains were selected for further analysis (**Supplementary Table 17a**). The 1,190 genomes were selected according to four criteria: completely sequenced genomes; genome of the type strain; longest genome among the same strains; different genomes at the species level that was determined by the comparison of the average nucleotide identity. Using these criteria, the genome of a single strain of a species was selected and used as the reference for the whole metagenomic read alignment. To identify existing genomes in the tomato rhizosphere, whole metagenomic reads were mapped to the 1,190 genomes using BWA with the parameter of 20 maximum edit distance⁵². For comparative analysis of TRG1 with *Flavobacteriia* genomes, 226 genomes including draft sequences of *Flavobacteriia* (**Supplementary Table 17b**) and TRG1 were used as reference for the whole metagenomic read alignment.

To reveal genomic features of TRG1, distinguishable from those of closely associated genomes, orthologous genes of *Gaetbulibacter saemankumensis* DSM 17032, *Bizionia argentinensis* JUB59, *Formosa* sp. AK20, *Mangrovimonas yunxiaonensis* LY01, *Gelidibacter mesophilus* DSM 14095, *Sediminibacter* sp. Hel_I_10, *Psychroserpens* sp. PAMC_27130, and *Psychroserpens* sp. Hel_I_66, which are the strains located in the same phylogenetic clade as TRG1, as well as orthologous genes of *F. daejeonense* RCH33 and *F. daejeonense* DSM 17708 were determined using OrthoMCL (version 2.0.3)⁶⁶ with parameters of e value $\leq 1 \times 10^{-5}$, identity $\geq 50\%$, and coverage $\geq 50\%$. COG distribution of the genomes was analyzed using RPS-BLAST with the parameter of an e value 1×10^{-2} . Analysis of carbohydrate active enzymes was performed using CAZymes Analysis Toolkit⁶⁶ with Pfam based annotation, and classification of transporter families was conducted with BLASTP against a transporter classification database⁶⁷.

In vitro isolation and cultivation of TRM1. The soil sample from Hawaii 7996 was used to isolate *Flavobacteriaceae* sp. TRM1 and three TRM1-specific primers were designed to detect it. Three marker genes—*rpoA*, *recA* and *secY*—were chosen for designing TRM1-specific primers. The *rpoA*, *recA* and *secY* genes from eight genomes (*Bizionia argentinensis* JUB59, *Formosa agariphila* KMM 3901, *Gaetbulibacter saemankumensis* DSM 17032, *Gelidibacter mesophilus* DSM 14095, *Mangrovimonas yunxiaonensis* LY01, *Psychroserpens* sp. Hel_I_66, *Sediminibacter* sp. Hel_I_10, and *Siansivirga zeaxanthinifaciens* CC-SAMT-1), as well as those of *F. daejeonense* RCH33, belonging to the family *Flavobacteriaceae*, were aligned with the corresponding genes in TRG1, and variable regions were examined to select TRM1-specific primer candidates. To ensure the specificity of each primer, candidate primers were searched against the NR database using BLASTN (**Supplementary Table 9a**). To analyze the metabolic features of TRM1, metabolic pathways were analyzed by KAAS (KEGG Automatic Annotation Server) using amino-acid sequences of TRG1.

To cultivate TRM1, approximately 2 g of Hawaii 7996 soil was inoculated into 1:10 (v/v) diluted marine broth (MB; Difco 2216, USA) containing 2% NaCl and incubated at 25 °C for 3 d. The enrichment culture was stored as a 50% glycerol stock at -80 °C. To identify the optimal growth medium for TRM1, cells from glycerol stock were inoculated into 1/10 MB, 1/10 MB supplemented with 0.2% D-mannose or 0.2% L-fucose, artificial seawater (ASW) supplemented with 0.5% peptone, and ASW supplemented with 0.5% peptone and 0.2% D-mannose or 0.2% L-fucose. The concentration of NaCl in each medium was 2%. After inoculation of cells from the glycerol stock into all six media, cells were harvested every 24 h and genomic DNA was extracted and adjusted to the same concentration. PCR of the genomic DNA was performed using TRM1-specific primers and a universal primer set (27F and 1492R) for the 16S rRNA gene.

To isolate TRM1, cells from the glycerol stock were inoculated into 1/10 MB containing 2% NaCl or ASW supplemented with 0.5% peptone and 0.2%

D-mannose, and incubated at 25 °C for 3 d. Cultured broth was spread onto an agar plate containing the same medium and cyclohexamide (1 µg/ml), and incubated at 25 °C for 6 d. Colonies grown on the plates were picked and subjected to colony PCR. Finally, candidate colonies of TRM1 were isolated from agar plates containing 1/10 MB, 2% NaCl, and 30 µg/ml kanamycin.

Cell morphology and anti-*R. solanacearum* effect of TRM1. For observation of the cell morphology of TRM1-10, bacterial colonies were grown on a marine agar (MA; Difco 2216, USA) plate at 30 °C for 4 d and cell suspension was acquired. Preparation of sample for scanning electron microscopy (SEM) and filming of s.e.m. images were performed at the Korea Research Institute of Bioscience and Biotechnology (KRIBB). Antagonistic activity of TRM1-10 against *R. solanacearum* *in vitro* was investigated as described above.

Evaluation of bacterial strains for suppression of bacterial wilt. Prevention of bacterial wilt progress by TRM1-10, three *Flavobacterium* strains (RC62, RCH33, and TCH3-2), and *Pseudomonas putida* KT2440 was investigated using Moneymaker. Surface sterilized tomato seeds were germinated in a pot with various soils and grown for 2 weeks before bacterial application. Sterilized or non-sterilized nursery media and the natural field soil collected from Dong-A University Agricultural Experimental Station were used to grow tomato plants. When natural field soil was used to grow tomato plants, the equal amount of non-sterilized commercial Horticulture Nursery Media (v/v) was mixed with natural field soil to improve drainage.

TRM1-10 was cultivated in MA plates at 30 °C for 4 d and prepared as bacterial suspension with sterile water to have various concentrations. The prepared bacterial suspensions were poured into a pot with tomato plants grown for 2 weeks to reach bacterial density at a concentration of 2×10^6 CFU/g soil, 2×10^7 CFU/g soil, and 2×10^8 CFU/g soil. *F. aquidurens* RC62 and *Flavobacterium* sp. TCH3-2 were incubated in TSA at 30 °C for 2 d; *F. daejeonense* RCH33 and *P. putida* KT2440 were cultured in TSA at 30 °C for 1 day. The cultured bacterial cells were suspended in sterilized distilled water, and optical density (OD) was adjusted to 0.5 at 600 nm which corresponded to 2.9×10^9 CFU/ml for RC62, 5.9×10^8 CFU/ml for TCH3-2, 5.4×10^8 CFU/ml for RCH33 and 3.4×10^9 CFU/ml for KT2440. Bacterial suspensions were adjusted to treat $2-6 \times 10^8$ CFU/g soil for each treatment. All treatments included ten plants for each experiment and included three replications. Non-treated plants were the negative control. 7 d after the application of TRM1-10, RC62, RCH33, TCH3-2, and KT2440, *R. solanacearum* SL341 was inoculated into the tomato plants by a soil-soaking method as described. Disease progress of bacterial wilt was examined for two more weeks after inoculation.

Enumeration of culturable cells by colony counting. To investigate the bacterial population of TRM1-10 and *R. solanacearum* SL341 in the tomato rhizosphere and bulk soil, tomato plants (cv. Hawaii 7996 and Moneymaker) grown in pots containing sterilized nursery media were treated with TRM1-10 and/or SL341. Seedlings germinated from surface-sterilized seeds were grown inside a growth chamber for three weeks, watered daily by sterilized distilled water, before bacterial treatment as shown in **Figure 6a**. Both cultivars of tomato were treated with TRM1-10 at a cell density of 2×10^8 CFU/g soil which was assessed to be the effective cell density for successfully suppressing the bacterial wilt incidence in a susceptible tomato cultivar, Moneymaker (**Fig. 5c**). TRM1-10 cell density was measured 3 h post treatment as the D0 reading. After seven days of TRM1-10 treatment, the plants were inoculated with SL341 at the cell density of 1×10^7 CFU/g soil. SL341 cell density was measured 3 h post inoculation (D7). The population density for TRM1-10 and SL341 were measured individually in the bulk and rhizosphere soil on the third and seventh days after SL341 inoculation as D10 and D14 readings, respectively.

TRM1-10 population was determined by the plate count method for viable cells. To collect the rhizosphere and bulk soils, each tomato plant (five replicates) was harvested from the pots. Soils were collected and weighed and subject to serial dilution in 0.75% saline buffer. Briefly, soil loosely adhering to the root was removed by gentle tapping and that firmly adhering to the root was collected by sonication at 135 W for 5 min (Branson 5500DTH, Danbury) in a saline buffer. The rhizosphere soil was obtained by centrifugation at 13,000 rpm for 15 min, and weighed for serial dilution. Serial dilutions from both rhizosphere and bulk soils were spread on prepared MA 2216

(BD) supplemented with 100 µg/ml of cycloheximide, 30 µg/ml of nystatin, 50 µg/ml of geneticin, 30 µg/ml of gentamicin, and 30 µg/ml of streptomycin and incubated at 30 °C to enumerate TRM1-10 colonies. The same suspensions were spread-plated on SMSA medium⁶⁸ to enumerate SL341 population. To investigate the *in planta* population of SL341, roots were excised below the hypocotyl and the root samples completely devoid of soil particles were washed in 10 ml of 80% ethanol for 30 s, followed by washing with 3% bleach. The roots were then extensively washed with sterilized distilled water, weighed and grinded using mortar and pestle, before spreading on SMSA to count CFU per gram of root fresh weight.

All statistical analyses were performed with the R software (version 3.4.0). Data were log-transformed to stabilize the variance and obtain normal distribution. The log-transformed CFU/g was examined using the Shapiro-Wilk normality test, subsequently two-sample, two-sided *t* test and one-way univariate analysis of variance (ANOVA) were conducted followed by Tukey's honestly significant difference (HSD) *post hoc* test ($P < 0.05$) for determining any significant difference between or among the samples. When two samples for comparison had unequal variances, we performed Welch's two-sample *t* test (Supplementary Table 13).

Quantification of bacterial DNA by quantitative real-time PCR. To quantify populations of TRM1-10 and SL341 in the rhizosphere of Hawaii 7996 and Moneymaker, quantitative PCR real-time (qPCR) assays were conducted. A gene (locus tag: TRG1_2767 in Supplementary Table 7) involved in cellulose biosynthesis was chosen as a target allele for designing a TRM1-specific primer pair. Primers TRM1-CBf and TRM1-CBr were developed after comparison of highly similar sequences from BLAST searches (Supplementary Table 9b). A specific primer set of SL341, 759 and 760 targeting the upstream region of UDP-3-O-acetyl-GlcNAc deacetylase gene, was selected from a previous study⁶⁹. Primer pairs were accessed as strain-specific since amplification was observed at a PCR reaction with DNA extracted from the target strain-spiked rhizosphere soil, which was not detected with DNA from non-target strain-spiked one. Quantitative PCR was performed by QuantStudio 3 Real-Time PCR System (Applied Biosystems) using Power SYBR green PCR master mix (Applied Biosystems). The cycling program included a 5 min pre-incubation at 95 °C, 40 cycles consisting of 95 °C for 15 s and 60 °C for 1 min for amplification with primer set TRM1-CBf/TRM1-CBr; 95 °C for 15 s and 56 °C for 15 s followed by 72 °C for 25 s for 759/760. Additional reaction on the PCR product by denaturing at 95 °C for 15 s, holding at 60 °C for 1 min, and ramping the temperature up to 95 °C at a rate of 0.15 °C/s was performed to yield a melting curve that was used to confirm the amplification specificity.

Amplification efficiencies of each primer set were calculated by generating standard curves by plotting the cycle threshold (C_T) value against the logarithm of the serially diluted DNA (10 fg to 10⁷ fg) isolated from target strains. qPCR data was analyzed with QuantStudio Design and Analysis Software v1.4.2. Amplification efficiencies with TRM1-10- and SL341-specific primers with bacterial cell culture are summarized in Supplementary Table 18. The standard curves used for the quantification of TRM1 and SL341 in the tomato rhizospheres were also generated. 200 mg of root-attached rhizosphere soil of 2-week-old Moneymaker were placed in tubes, and spiked with 1 ml of each bacterial culture in quantities ranging from 10³ to 10⁸ CFU/ml, and tubes were vortexed and then incubated for 2 h at 25 °C. DNA was extracted from the whole mixture with a FastDNA spin kit for soil (MP Biomedicals). Subsequently, qPCRs with 2 µl of extracted DNA and TRM1-10- or SL341-specific primers was performed as described above. Standard curves were generated by plotting the C_T number versus the logarithm of bacterial DNA concentration, which was converted to CFU for each spiked bacterial amount. Calculated amplification efficiencies with DNA purified from rhizosphere soil spiked with TRM1 and SL341 are as shown in Supplementary Table 18. To enumerate the number of CFU of TRM1 and SL341 in the rhizosphere, the same rhizosphere soil mixtures used for colony counting assay at indicated time points in Figure 6a. DNA of each samples were extracted by the FastDNA

spin kit, the amount of DNA was interpolated via C_T value from the linear regression line through the standard data points, and the qPCR quantification data was converted to the equivalent number of CFU per gram of rhizosphere soil. Statistical analyses were performed by using the R software (version 3.4.0). In comparison of the quantification data between the Hawaii 7996 and Moneymaker rhizospheres, or between the two SL341-spiked Moneymaker rhizospheres, two-sample *t* test or Welch's two-sample *t* test were used. Mean comparisons among many TRM1-treated plant rhizospheres were performed by ANOVA and the Tukey's HSD *post hoc* test (Supplementary Table 13). Correlation between colony counts and qPCR results were assessed by Pearson correlation analysis.

Data availability. The sequences used in this study were deposited in GenBank under BioProject number PRJNA295927, which comprises 17 SRA files for pyrosequencing reads of the 16S rRNA gene for Hawaii 7996, Moneymaker, Korean cabbage and bulk soil, two FASTA files for the scaffolds generated from Illumina shotgun sequencing of the whole metagenome for Hawaii 7996 and Moneymaker at the first sampling, and the sequence of TRG1 assembled from the metagenomic reads of Hawaii 7996. The accession number for TRG1 is LKLA01.

51. Thoquet, P. *et al.* Quantitative trait loci determining resistance to bacterial wilt in tomato cultivar Hawaii 7996. *Mol. Plant Microbe Interact.* **9**, 826–836 (1996).
52. Human Microbiome Project Consortium. Structure, function and diversity of the healthy human microbiome. *Nature* **486**, 207–214 (2012).
53. Lan, Y., Wang, Q., Cole, J.R. & Rosen, G.L. Using the RDP classifier to predict taxonomic novelty and reduce the search space for finding novel organisms. *PLoS One* **7**, e32491 (2012).
54. Jonsson, V., Österlund, T., Nerman, O. & Kristiansson, E. Statistical evaluation of methods for identification of differentially abundant genes in comparative metagenomics. *BMC Genomics* **17**, 78 (2016).
55. Heo, J. *et al.* Gut microbiota modulated by probiotics and *Garcinia cambogia* extract correlate with weight gain and adipocyte sizes in high fat-fed mice. *Sci. Rep.* **6**, 33566 (2016).
56. Robinson, M.D., McCarthy, D.J. & Smyth, G.K. edgeR: a Bioconductor package for differential expression analysis of digital gene expression data. *Bioinformatics* **26**, 139–140 (2010).
57. Zhu, W., Lomsadze, A. & Borodovsky, M. *Ab initio* gene identification in metagenomic sequences. *Nucleic Acids Res.* **38**, e132 (2010).
58. Li, W. & Godzik, A. Cd-hit: a fast program for clustering and comparing large sets of protein or nucleotide sequences. *Bioinformatics* **22**, 1658–1659 (2006).
59. Mavromatis, K. *et al.* The DOE-JGI standard operating procedure for the annotations of microbial genomes. *Stand. Genomic Sci.* **1**, 63–67 (2009).
60. Kong, H.G. *et al.* Induction of the viable but nonculturable state of *Ralstonia solanacearum* by low temperature in the soil microcosm and its resuscitation by catalase. *PLoS One* **9**, e109792 (2014).
61. Roberts, D.P., Denny, T.P. & Schell, M.A. Cloning of the *egl* gene of *Pseudomonas solanacearum* and analysis of its role in phytopathogenicity. *J. Bacteriol.* **170**, 1445–1451 (1988).
62. Reasoner, D.J. & Geldreich, E.E. A new medium for the enumeration and subculture of bacteria from potable water. *Appl. Environ. Microbiol.* **49**, 1–7 (1985).
63. Lamprecht, A.L. *et al.* GeneFisher-P: variations of GeneFisher as processes in Bio-jETI. *BMC Bioinformatics* **9**(Suppl. 4), S13 (2008).
64. Dupont, C.L. *et al.* Genomic insights to SAR86, an abundant and uncultivated marine bacterial lineage. *ISME J.* **6**, 1186–1199 (2012).
65. Bowers, R.M. *et al.* Minimum information about a single amplified genome (MISAG) and a metagenome-assembled genome (MIMAG) of bacteria and archaea. *Nat. Biotechnol.* **35**, 725–731 (2017).
66. Park, B.H., Karpinets, T.V., Syed, M.H., Leuze, M.R. & Uberbacher, E.C. CAZymes Analysis Toolkit (CAT): web service for searching and analyzing carbohydrate-active enzymes in a newly sequenced organism using CAZy database. *Glycobiology* **20**, 1574–1584 (2010).
67. Saier, M.H. Jr., Reddy, V.S., Tamang, D.G. & Västermark, A. The transporter classification database. *Nucleic Acids Res.* **42**, D251–D258 (2014).
68. Schaad, N.W., Jones, J.B. & Chun, W. *Laboratory guide for identification of plant Pathogenic bacteria* (American Phytopathological Society Press, St. Paul, USA, 2001).
69. Opina, N. *et al.* A novel method for development of species and strain specific DNA probes and PCR primers for identifying *Burkholderia solanacearum* (formerly *Pseudomonas solanacearum*). *Asia Pac. J. Mol. Biol. Biotechnol.* **5**, 19–30 (1997).

Reporting Summary

Nature Research wishes to improve the reproducibility of the work that we publish. This form provides structure for consistency and transparency in reporting. For further information on Nature Research policies, see [Authors & Referees](#) and the [Editorial Policy Checklist](#).

Statistical parameters

When statistical analyses are reported, confirm that the following items are present in the relevant location (e.g. figure legend, table legend, main text, or Methods section).

n/a Confirmed

- ☐ ☒ The exact sample size (n) for each experimental group/condition, given as a discrete number and unit of measurement
- ☐ ☒ An indication of whether measurements were taken from distinct samples or whether the same sample was measured repeatedly
- ☐ ☒ The statistical test(s) used AND whether they are one- or two-sided
Only common tests should be described solely by name; describe more complex techniques in the Methods section.
- ☒ ☐ A description of all covariates tested
- ☐ ☒ A description of any assumptions or corrections, such as tests of normality and adjustment for multiple comparisons
- ☐ ☒ A full description of the statistics including central tendency (e.g. means) or other basic estimates (e.g. regression coefficient) AND variation (e.g. standard deviation) or associated estimates of uncertainty (e.g. confidence intervals)
- ☐ ☒ For null hypothesis testing, the test statistic (e.g. F , t , r) with confidence intervals, effect sizes, degrees of freedom and P value noted
Give P values as exact values whenever suitable.
- ☒ ☐ For Bayesian analysis, information on the choice of priors and Markov chain Monte Carlo settings
- ☐ ☒ For hierarchical and complex designs, identification of the appropriate level for tests and full reporting of outcomes
- ☐ ☒ Estimates of effect sizes (e.g. Cohen's d , Pearson's r), indicating how they were calculated
- ☐ ☒ Clearly defined error bars
State explicitly what error bars represent (e.g. SD, SE, CI)

Our web collection on [statistics for biologists](#) may be useful.

Software and code

Policy information about [availability of computer code](#)

Data collection

Provide a description of all commercial, open source and custom code used to collect the data in this study, specifying the version used OR state that no software was used.

Data analysis

We used R for statistical analyses. Other software packages used include Mothur pipeline, CLC Genomics Workbench, CLC Assembly Cell, CD-HIT, UCHIME, BLAST, BMTagger, MetaGeneMark, BWA, Multimetagenome pipeline, R package, OrthoMCL.

For manuscripts utilizing custom algorithms or software that are central to the research but not yet described in published literature, software must be made available to editors/reviewers upon request. We strongly encourage code deposition in a community repository (e.g. GitHub). See the Nature Research [guidelines for submitting code & software](#) for further information.

Data

Policy information about [availability of data](#)

All manuscripts must include a [data availability statement](#). This statement should provide the following information, where applicable:

- Accession codes, unique identifiers, or web links for publicly available datasets
- A list of figures that have associated raw data
- A description of any restrictions on data availability

The sequences used in this study were deposited in GenBank under BioProject number PRJNA295927, which comprises seventeen SRA files for pyrosequencing reads, two FASTA files for the scaffolds generated from Illumina shotgun sequencing, and the sequence of TRG1.

Field-specific reporting

Please select the best fit for your research. If you are not sure, read the appropriate sections before making your selection.

☒ Life sciences ☐ Behavioural & social sciences ☐ Ecological, evolutionary & environmental sciences

For a reference copy of the document with all sections, see [nature.com/authors/policies/ReportingSummary-flat.pdf](https://www.nature.com/authors/policies/ReportingSummary-flat.pdf)

Life sciences study design

All studies must disclose on these points even when the disclosure is negative.

Sample size	Sample sizes of Fig. 2b (transplant) and Fig. 5c (TRM1-10) for the disease progress curve of bacterial wilt: three independent replications and 5-10 plants per each replicate. Fig. 2b is a result of 18-20 plants per treatment after replantation or transplantation and Fig. 5c is a result of 30 plants per treatment. Those replicates are optimal sampling size representing each population for bacterial wilt progress. Sample size of Fig. 6 for bacterial population dynamics was five replicates (plants) and three readings per each replicate. Three to four replicates are usual for population experiments.
Data exclusions	We did not exclude any data for our analyses.
Replication	Transplant experiments (Fig. 2b) were replicated 2 or 3 times to reproduce virtually similar results, and the effect of TRM1-10 on bacterial wilt (Fig. 5c) and bacterial population dynamics (Fig. 6) were replicated twice to reproduce similar results.
Randomization	Experimental sets for the replicates of Fig. 2b, Fig. 5c, and Fig. 6 were allocated randomly.
Blinding	Complete blinding for data collection was not necessary for Fig. 2b, Fig. 5c, and Fig. 6, because we investigated the disease severity of individual plant daily after pathogen challenge. However, individual plant constituting technical replicates was randomly numbered to be partially blind.

Reporting for specific materials, systems and methods

Materials & experimental systems

n/a	Involved in the study
<input checked="" type="checkbox"/>	<input type="checkbox"/> Unique biological materials
<input checked="" type="checkbox"/>	<input type="checkbox"/> Antibodies
<input checked="" type="checkbox"/>	<input type="checkbox"/> Eukaryotic cell lines
<input checked="" type="checkbox"/>	<input type="checkbox"/> Palaeontology
<input checked="" type="checkbox"/>	<input type="checkbox"/> Animals and other organisms
<input checked="" type="checkbox"/>	<input type="checkbox"/> Human research participants

Methods

n/a	Involved in the study
<input checked="" type="checkbox"/>	<input type="checkbox"/> ChIP-seq
<input checked="" type="checkbox"/>	<input type="checkbox"/> Flow cytometry
<input checked="" type="checkbox"/>	<input type="checkbox"/> MRI-based neuroimaging